Assessing the dynamics of Lassa fever with impact of environmental sanitation: optimal control and cost-effectiveness analysis

Afeez Abidemi[a,b], Kolade M. Owolabi[a,b,*], Edson Pindza[c]

[a] *Department of Mathematical Sciences, Federal University of Technology, Akure, P.M.B. 704, Ondo State, Nigeria*
[b] *ORCID iD: 0000-0003-1960-0658 (AA); 0000-0001-9290-3458 (KMO)*
[c] *Department of Mathematics and Applied Mathematics, University of Pretoria, Pretoria 002, South Africa*

Abstract

This study discusses the development and analysis of a nonlinear optimal control problem for a Lassa fever (LF) deterministic model featuring vertical transmission route, nonlinear form of incidence terms and effect of environmental sanitation with a view to providing insightful information to the government, decision and policy makers about how to prioritize the implementations of environmental fumigation, use of condom, use of antiviral therapy, rodent reduction control and educational campaign in terms of efficacy and cost benefits. An existing seven-dimensional deterministic model of LF dynamics is extended to take into account five time-dependent control variables accounting for environmental fumigation, use of condom, use of antiviral therapy, rodent reduction control and educational campaign. Optimal control theory with the aid of Pontryagin's maximum principle is employed to derive the necessary conditions for the existence of optimal control quintuple. To investigate how the implementation of various single, double, triple, quadruple and quintuple control interventions minimize LF spread in the population at minimum cost, numerical experiment is conducted on the derived optimality system. More importantly, efficiency analysis is carried out to ascertain the most efficient interventions among the set of different control strategies under consideration. While cost-effectiveness analysis is done to determine the least costly control intervention that can be implemented to nip the spread of LF in the population.

Keywords: Cost-effectiveness analysis, Efficiency analysis, Lassa fever transmission, Optimal control Lassa fever model, Incremental cost-effectiveness ratio

2010 MSC: 37C60, 49M05, 92D30, 93A30

1. Introduction

Lassa fever (LF) is a zoonotic disease associated with acute and potentially fatal haemorrhagic disease caused by Lassa virus (LASV), a member of the *Arenaviridae* virus family (Eberhardt et al., 2019; Wiley et al., 2019; Yaro et al., 2021). LASV was first discovered in Nigeria in 1969 (Wiley et al., 2019; Mari Saez et al., 2018) and later detected in Liberia in 1972 (Wiley et al., 2019). The virus is now endemic in several West African countries (Eberhardt et al., 2019; Tuite et al., 2019) and occurs sporadically as well as in annual outbreaks (Eberhardt et al., 2019). Most of the confirmed LF cases are from Guinea, Liberia and Sierra Leone (the Mano River Union region)

*Corresponding author
Email addresses: aabidemi@futa.edu.ng (Afeez Abidemi), kmowolabi@futa.edu.ng (Kolade M. Owolabi), pindzaedson@yahoo.fr (Edson Pindza)

and Nigeria (Wiley et al., 2019; Yaro et al., 2021; Bell-Kareem and Smither, 2021; Purushotham et al., 2019), although the disease has also been detected in other countries including Benin, Burkina Faso, Ghana, Côte d'Ivoire, Mali, and Togo (Wiley et al., 2019; Purushotham et al., 2019), Central African Republic, Mali, Senegal and Congo (Yaro et al., 2021; Purushotham et al., 2019).

Worldwide, LF is regarded the most consequential rodent-borne virus infection (Smither and Bell-Kareem, 2021). Recognition of the disease as an important rodent-borne viral haemorrhagic fever is on the increase as it is presenting a severe public health threat to some of the communities in the affected West African countries (Zhao et al., 2020). Several factors, including reoccurring outbreaks, extensive domestic and international trade and civil unrest, have made LASV an emerging virus of upmost importance (Bell-Kareem and Smither, 2021). LF is associated with significant morbidity and mortality (Yaro et al., 2021), estimated to cause up to 300 thousand cases and 5 thousand deaths annually in West Africa regions where the disease is endemic (Eberhardt et al., 2019; Wiley et al., 2019; Yaro et al., 2021; Smither and Bell-Kareem, 2021) with about 58 million people at risk (Yaro et al., 2021).

The routes of transmission of LF include rodent to human, human to rodent, rodent to rodent, human to human and environment to human (Abdulhamid et al., 2022). The rodent *Mastomys natalensis*, a common households' rat in West Africa, is regarded the natural host/reservoir of LASV (Mari Saez et al., 2018; Tuite et al., 2019). However, there are newly reported hosts of LASV in Nigeria and Guinea Republic, namely, *Mastomys erythroleucus* (Guinea multimammate mouse) and *Hylomyscus pamfi* (African wood mouse) (Eberhardt et al., 2019; Mari Saez et al., 2018). These rodents are infected in utero and remain infectious until death (Asogun et al., 2019). In them, LASV exhibits persistent and asymptomatic infection (Purushotham et al., 2019). The LASV-infected rodents shed the virus in their urine and faeces. Human's primary infection takes place via direct or indirect contact with LASV-infected rodents. Those people living in rural areas where *Mastomys* rodents are commonly found, particularly in communities with poor sanitation or crowded living conditions, are at greatest risk of acquiring LASV infection (Asogun et al., 2019). Individuals contract LASV through direct contact with the excretions of rat such as urine and faeces, eating of contaminated food, inhalation of aerosolized urine in droplets or dust particles, consumption of the rat (Mari Saez et al., 2018; Smither and Bell-Kareem, 2021) and being bitten by the rodents (Mari Saez et al., 2018). The occurrence of this human-vector interface is predominant in resource-limited communities where health care and laboratory diagnostic testing are not easily accessible (Purushotham et al., 2019).

Secondary human to human transmission occurs in both the community and health care settings (Mari Saez et al., 2018). This mode of the disease spread among individuals has been recorded in people in the community with overcrowded living conditions, families in the course of providing health care for their sick person as well as in communities in the context of burial practices (Asogun et al., 2019). Direct contact with blood or bodily fluids (such as urine and semen) of infected individuals can also lead to human to human transmission of LASV (Yaro et al., 2021; Tuite et al., 2019), thereby posing risk of sexual transmission (Yaro et al., 2021). Sexual transmission occurring months after recovery from LASV infection has been documented (Asogun et al., 2019). Moreover, health care workers are at high risk of LASV infection. Nosocomial transmission of LASV occurs within hospitals among and between patients and health care workers. This usually occurs due to poor adherence to the disease prevention and control practices. Inadequate barrier nursing and infection control practices also contribute majorly to the disease transmission in health care facilities (Asogun et al., 2019).

In humans, LASV is responsible for a wide spectrum of disease manifestations, ranging from asymptomatic cases to acute and severe cases. Onset of acute LF is gradual and non-specific, often begins with intermittent fever and malaise followed by myalgia, sore throat, facial oedema and severe headache. The virus has an incubation period usually 7 to 10 days, with a range of 3 to 21 days (Yaro et al., 2021). After primary LASV infection, signs and symptoms of LF manifest up to 21 days (Asogun et al., 2019). Recovery begins 8 to 10 days after disease onset in a mild case of LASV infection (Purushotham et al., 2019; Gibb et al., 2017), while fatal cases progress to shock, organ failure and death, sometimes with haemorrhagic manifestations (Gibb et al., 2017). Advanced life support is required when fatal cases progress to shock (Asogun et al., 2019). The mortality rate of LF is low, between 1 to 2%, in communities of endemic areas (Mari Saez et al., 2018; Zhao et al., 2020). Most cases are mild (or asymptomatic) and do not result in hospitalisation (Eberhardt et al., 2019; Mari Saez et al., 2018). The case fatality rate is approximately 20% amongst hospitalised patients and increases to above 50% in high risk groups, including pregnant women and infants. In pregnant women, the severe case of LF results into almost 100% mortality in foetuses (Purushotham et al., 2019).

Up to date, no vaccines have been licensed against LASV (Yaro et al., 2021). Antiviral treatment options for LF are limited, with ribavirin considered to be effective when given early in the course of disease (between the first six days counting from after the onset of the symptoms) to improve survival in LF patients (Mari Saez et al., 2018). Using ribavirin can reduce the mortality risk to below 5% if administered early, whereas the benefits are greatly diminished if the drug is started later in the course of disease (Purushotham et al., 2019). Also, nosocomial case fatality and transmission can be reduced by treating patients with LF in dedicated treatment wards with facilities for enhanced supportive care such as dialysis and respiratory support (Asogun et al., 2019). Thus, rodent control and human behavioural changes are currently the main options available to prevent LF in highly endemic areas (Mari Saez et al., 2018). Avoiding contact with *Mastomys* rodents can reduce the risk of primary transmission of LASV to humans (Yaro et al., 2021). Placing food away in rodent-proof containers, ensuring clean homes and surroundings and trapping in and around homes can be helpful to decrease rodent population and human contact with rodents droppings or urine. Further, risk of LASV infection can be reduced by educating people, especially those in high-risk areas, about ways to reduce the population of rodent in their homes and surroundings. The spread of human LASV infection in health care settings can be prevented through mandatory strict adherence to standard infection prevention and control precautions by health care workers (Asogun et al., 2019).

In several works, many mathematicians have studied nonlinear mathematical models governed by autonomous systems of ordinary differential equations (ODEs) to facilitate understanding of the epidemiology of infectious diseases (e.g., see Naik et al. (2020); Paul and Kuddus (2022); Anggriani and Beay (2022); Asma et al. (2022); Abidemi and Aziz (2022); Alade (2021); Mishra et al. (2020) and some of the references therein). In few studies, the technique of mathematical modelling has been applied to influence the decision-making processes as regard the intervention programs for prevention and control of LF transmission dynamics in the community (Abdulhamid et al., 2022; Abidemi et al., 2022b; Abdullahi, 2021; Alkahtani and Alzaid, 2020; Atangana, 2015; Faniran and Ayoola, 2022; Goyal et al., 2019; Jain and Atangana, 2018; Lingas et al., 2021; Barua et al., 2021; Ogunmiloro, 2022).

The application of optimal control theory to infectious disease modelling provides insightful information about

how the optimal implementation of control interventions can be achieved. Since the application of optimal control theory to disease modelling, there is a significant number of researches in the literature of mathematical modelling of infectious diseases that make use of optimal control theory concept (Falowo et al., 2022; Asamoah et al., 2020, 2022; Cantor and Ganiats, 1999). However, despite that optimal control theory has provided useful epidemiological insights in ascertaining the optimal control interventions needed to minimize the dynamics of disease transmission in the community at minimum cost of implementation, the number of studies that have made use of mathematical modelling approach to investigate the optimal control of LF transmission dynamics in the literature of mathematical epidemiology is limited (Peter et al., 2020; Higazy et al., 2021; Onah et al., 2020; Ojo et al., 2022; Ibrahim et al., 2021; Musa et al., 2022). For instance, Peter et al. (2020) developed seven-dimensional non-optimal control and optimal control compartmental models for LF transmission dynamics. Four control variables were incorporated into the optimal control model to account for fumigation of the environment with pesticide, condom usage, early supportive treatment for infected individuals, and indoor residual spray. To explicitly derive the necessary conditions for the optimal control quadruple, Pontryagin's maximum principle (PMP) was employed by the authors.

Higazy et al. (2021) constructed a 4-dimensional deterministic fractional-order optimal control model to describe the dynamics of LF in pregnant woman population. Furthermore, the authors in Onah et al. (2020) have presented and analysed both non-optimal control and optimal control mathematical models describing the transmission dynamics of LF in the interacting human and rodent populations. Stability theory of differential equations was used for detailed stability analysis of the non-optimal control model. Moreover, the optimal control model was analysed to derive the cost benefits associated with implementing optimal rodent control, external protection, treatment and isolation interventions for the minimization of LF transmission dynamics at minimum cost. Recently, Ojo et al. (2022) developed and analysed a nonlinear optimal control LF model including four time-dependent controls, namely, educational campaign policy, use of condom, treatment control and use of rodents trap. The authors further explored cost-effectiveness analysis to ascertain the most cost-effective strategy among the various optimal control combination strategies implemented in the study. In a related development, Ibrahim et al. (2021) studied a nonlinear optimal control model of LF dynamics which takes into account public awareness, standard precautions in treatment and environmental sanitation as time-dependent control variables. Musa et al. (2022) proposed an optimal control model to assess the optimal use of proper sanitation and personal hygiene for exposed individuals and adequate health resources for mild infectious individuals required for an effective management of LF transmission in the community.

According to Abidemi et al. (2022b), none of the previously existing studies of LF transmission dynamics captured vertical transmission (particularly mother to child transmission) route in human population, and hence their work in Abidemi et al. (2022b) was the first to attempt to consider the effect of vertical transmission route in human population in the formulation of the model presented by the authors. In addition, their model used a simple approach to capture the effect of socio-economic factors like community hygiene through environmental sanitation. A nonlinear mathematical epidemic model that features both vertical (including mother to child transmission) and horizontal modes of transmission provides a foundation for the application of control intervention (Abidemi et al., 2022b). In view of this, the work of Abidemi et al. (2022b) provides a more realistic mathematical modelling framework for optimal control of the transmission dynamics of LF in the population. Hence, this paper aims at

constructing and analysing a nonlinear optimal control LF transmission model featuring both vertical and horizontal transmission routes, effect of socio-economic factors and nonlinear incidence functions. The new nonlinear optimal control LF model, which is motivated by the work of Abidemi et al. (2022b), is developed by including five time-dependent control functions accounting for environmental fumigation, use of condom, use of antiviral therapy, rodent reduction control and educational campaign. Analysis of the new optimal control model is carried out by employing optimal control theory. It is imperative to emphasize that the optimal control LF model proposed in this work is novel compared to the existing optimal control LF models (Peter et al., 2020; Higazy et al., 2021; Onah et al., 2020; Ojo et al., 2022). It can be seen that none of the aforementioned studies considered up to five time-dependent control interventions in the model analysis. To the best of our knowledge, this work is the first to attempt to explicitly consider educational campaign (such as enforcement of regular environmental sanitation) on susceptible individuals with poor community hygiene as part of LF integrated control strategy.

The rest of this work is structured as follows. In Sect. 2, introduction to the non-optimal control LF transmission model previously studied by Abidemi et al. (2022b) is made in brief. Section 3 is devoted to the development and analysis of a new nonlinear optimal control LF model. Simulations of the optimality system emanating from the theoretical analysis are carried out in Sect. 4. Efficiency and cost-effectiveness analyses are also conducted in this section. Section 5 is concerned with the presentation of the results of numerical analysis of the optimal control LF model as well as the efficiency and cost-effectiveness analyses. In Sect. 6, results are discussed in detail. Finally, Sect. 7 gives the concluding remarks.

2. Non-optimal control LF transmission model

In Abidemi et al. (2022b), the authors studied a nonlinear mathematical model governed by a 7-dimensional system of ODEs describing LF transmission dynamics. The model stratifies the total human population, N_h, into five epidemiological classes, namely, susceptible individuals with good community hygiene (S_{h_1}), susceptible individuals with poor community hygiene (S_{h_2}), infected and infectious individuals (I_h), treated (or hospitalized) individuals (T_h) and recovered individuals with temporary immunity (R_h). The total rodent (reservoir) population, N_r, is made up of susceptible rodents (S_r) and infected and infectious rodents (I_r). The non-linear mathematical model for LF transmission dynamics between the interacting human and rodent populations, which was studied in

depth by the authors in Abidemi et al. (2022b), is given as

$$\begin{aligned}
\frac{dS_{h_1}}{dt} &= (1-\sigma)\Lambda_h + \pi\phi_h R_h + \psi_h S_{h_2} - \epsilon(1-\nu)\Lambda_h I_h - \eta\left(\frac{\beta_h I_h}{1+\alpha_1 I_h} + \frac{\beta_{rh} I_r}{1+\alpha_2 I_r}\right) S_{h_1} - \mu_h S_{h_1},\\
\frac{dS_{h_2}}{dt} &= \sigma\Lambda_h + (1-\pi)\phi_h R_h - \epsilon\nu\Lambda_h I_h - \left(\frac{\beta_h I_h}{1+\alpha_1 I_h} + \frac{\beta_{rh} I_r}{1+\alpha_2 I_r}\right) S_{h_2} - \mu_h S_{h_2} - \psi_h S_{h_2},\\
\frac{dI_h}{dt} &= \epsilon\Lambda_h I_h + \left(\frac{\beta_h I_h}{1+\alpha_1 I_h} + \frac{\beta_{rh} I_r}{1+\alpha_2 I_r}\right)(\eta S_{h_1} + S_{h_2}) - (\alpha_h + \gamma_h + \mu_h + \delta_h) I_h,\\
\frac{dT_h}{dt} &= \alpha_h I_h - \theta\sigma_h T_h - (1-\theta)\delta_h T_h - \mu_h T_h,\\
\frac{dR_h}{dt} &= \gamma_h I_h + \theta\sigma_h T_h - (\phi_h + \mu_h) R_h,\\
\frac{dS_r}{dt} &= \Lambda_r - \frac{\beta_{hr} S_r I_h}{1+\alpha_1 I_h} - \frac{\beta_r S_r I_r}{1+\alpha_2 I_r} - \mu_r S_r,\\
\frac{dI_r}{dt} &= \frac{\beta_{hr} S_r I_h}{1+\alpha_1 I_h} + \frac{\beta_r S_r I_r}{1+\alpha_2 I_r} - \mu_r I_r,
\end{aligned} \tag{1}$$

with initial conditions given as

$$x(0) = x_0, \text{ where } x = (S_{h_1}, S_{h_2}, I_h, T_h, R_h, S_r, I_r). \tag{2}$$

It should be noted that the population dynamics for each of the compartments of the non-optimal control LF model (1) has been well-discussed in Abidemi et al. (2022b). However, for convenience, the full descriptions of all the parameters of model (1), as done by Abidemi and co-workers in Abidemi et al. (2022b), are reproduced as shown in Table 1. Also, it is important to state that detailed analysis of the non-optimal control LF model (1) has been conducted in Abidemi et al. (2022b). Thus, we explore the optimal control version of the model in the next section.

3. Formulation of optimal control LF transmission model and its theoretical analysis

3.1. Formulation of optimal control LF transmission model

In view of the insightful results arising from the sensitivity analysis carried out on model (1) by Abidemi et al. (2022b), we introduce five different time-dependent control variables $u_i(t)$, where $i = 1, 2, \ldots, 5$, into the basic model (1). The control variables are discussed as follows:

(i) $u_1(t)$ represents the control variable for environmental fumigation with pesticide, which is targeted towards the prevention of rodent to human LF transmission.

(ii) $u_2(t)$ denotes the control function to reduce the secondary human to human transmission of LASV. This can be achieved through the use of condom during sexual activities.

(iii) $u_3(t)$ denotes the control variable for antiviral therapy to step up the management of symptomatic infected individuals in order to ensure prompt recovery and prevent deaths as a result of complications. Achievement of this is possible by providing a timely supportive treatment with the antiviral drug ribavirin.

(iv) $u_4(t)$ represents the control variable aimed at reducing the rodent population. This can be achieved through the use of indoor residual spray and rodents trap.

Table 1: Descriptions of parameters of model (1)

Parameter	Description
Λ_h	Rate of recruitment into susceptible human subpopulations through birth
η	Modification parameter on susceptible individuals with good hygiene
β_h	Effective transmission rate of LASV from human to human
β_{hr}	Effective transmission rate of LASV from human to rat
ϵ	Rate of vertical transmission of LASV
μ_h	Natural death rate of humans
δ_h	LF-induced death rate in human population
ψ_h	Proportion of S_{h_2} with improved community sanitation
α_1, α_2	Saturation constants
θ	Proportion of treated humans that recovers due to treatment
$1-\theta$	Proportion of treated humans that die of LF
$1-\nu$	Proportion of S_{h_1} with vertical transmission of LASV
ν	Proportion of S_{h_2} with vertical transmission of LASV
α_h	Rate of treatment of symptomatic infectious humans
$1-\sigma$	Proportion of humans recruited into class S_{h_1}
σ	Proportion of humans recruited into class S_{h_2}
σ_h	Recovery rate of treated humans
γ_h	Recovery rate of infected and infectious humans by natural immunity
ϕ_h	Relapse rate for individuals in class R_h
π	Proportion of individuals in class R_h that enter class S_{h_1} due to relapse
$1-\pi$	Proportion of individuals in class R_h that loses immunity and enter class S_{h_2} again
Λ_r	Rate of recruitment of rodents through birth
β_r	Effective transmission rate of LASV from rodent to rodent
β_{rh}	Effective transmission rate of LASV from rat to human
μ_r	Natural death rate of rodents

(v) $u_5(t)$ accounts for educational campaign to promote good community or personal hygiene. This is achievable through the enforcement of timely and proper environmental sanitation on the susceptible individuals with poor hygiene.

After incorporating the five time-dependent controls $u_i(t)$ $(i = 1, 2, \ldots, 5)$ into the non-optimal control LF model

(1), the optimal control version of the model becomes

$$\begin{aligned}
\frac{dS_{h_1}}{dt} &= (1-\sigma)\Lambda_h + \pi\phi_h R_h + u_5(t)S_{h_2} - \epsilon(1-\nu)\Lambda_h I_h - \eta\left(\frac{(1-u_2(t))\beta_h I_h}{1+\alpha_1 I_h} + \frac{(1-u_1(t))\beta_{rh} I_r}{1+\alpha_2 I_r}\right) S_{h_1} - \mu_h S_{h_1},\\
\frac{dS_{h_2}}{dt} &= \sigma\Lambda_h + (1-\pi)\phi_h R_h - \epsilon\nu\Lambda_h I_h - \left(\frac{(1-u_2(t))\beta_h I_h}{1+\alpha_1 I_h} + \frac{(1-u_1(t))\beta_{rh} I_r}{1+\alpha_2 I_r}\right) S_{h_2} - \mu_h S_{h_2} - u_5(t)S_{h_2},\\
\frac{dI_h}{dt} &= \left(\frac{(1-u_2(t))\beta_h I_h}{1+\alpha_1 I_h} + \frac{(1-u_1(t))\beta_{rh} I_r}{1+\alpha_2 I_r}\right)(\eta S_{h_1} + S_{h_2}) + \epsilon\Lambda_h I_h - (\alpha_h + \gamma_h + \tau_1 u_3(t) + \mu_h + \delta_h)I_h,\\
\frac{dT_h}{dt} &= \alpha_h I_h - \theta\sigma_h T_h - (1-\theta)\delta_h T_h - \mu_h T_h,\\
\frac{dR_h}{dt} &= (\gamma_h + \tau_1 u_3(t))I_h + \theta\sigma_h T_h - (\phi_h + \mu_h)R_h,\\
\frac{dS_r}{dt} &= \Lambda_r - \frac{(1-u_1(t))\beta_{hr} S_r I_h}{1+\alpha_1 I_h} - \frac{(1-u_1(t))\beta_r S_r I_r}{1+\alpha_2 I_r} - (\mu_r + \tau_2 u_4(t))S_r,\\
\frac{dI_r}{dt} &= \frac{(1-u_1(t))\beta_{hr} S_r I_h}{1+\alpha_1 I_h} + \frac{(1-u_1(t))\beta_r S_r I_r}{1+\alpha_2 I_r} - (\mu_r + \tau_2 u_4(t))I_r,
\end{aligned} \tag{3}$$

with initial conditions given at time $t = 0$. In the optimal control model (3), τ_1 denotes the recovery rate of the symptomatic infectious individuals induced by antiviral therapy, while τ_2 is the rodents mortality rate induced by the rodent reduction control. Our goal is to minimize the cost functional

$$C(u_1, u_2, u_3, u_4, u_5) = \int_0^{t_f} \left(A_1 I_h + A_2(S_r + I_r) + \frac{1}{\rho}\sum_{i=1}^{5} B_i u_i^{\rho}(t)\right) dt \tag{4}$$

constrained by the state system (3), where A_1 and A_2 are positive weight constants for symptomatic infectious humans and total rodent (reservoir) population, respectively, $B_i > 0,\ i = 1, 2, \ldots, 5$, are the respective balancing weights for the controls $u_i, i = 1, 2, \ldots, 5$, the terms $\frac{1}{\rho}\sum\limits_{i=1}^{5} B_i u_i^{\rho}(t)$ define the cost control functions for environmental fumigation, condom use, use of antiviral therapy, rodent reduction control and educational campaign, respectively, $\rho \in \{1/2, 1, 2, \ldots, n\}$, t_f denotes the expected final time for implementation of the control interventions such that $t \in [0,\ t_f]$. Notably, ρ defines the nature of control terms in the pay-off. For instance, setting $\rho = 1$ corresponds to linear control terms in the pay-off leading to bang-bang controls. At $\rho = 2$, there correspond quadratic control terms in the pay-off implying continuous controls. To comply with standard in many literature on mathematical models of infectious diseases involving optimal control problems (for example, see Falowo et al. (2022); Asamoah et al. (2022); Peter et al. (2020); Ojo et al. (2022) and some of the references cited therein), ρ is fixed at $\rho = 2$.

Of particular interest is to find an optimal control quintuple, $u^* = (u_i^*),\ i = 1, 2, \ldots, 5$, such that

$$C(u^*) = \min_{U} \{C(u_i),\ i = 1, 2, \ldots, 5\}, \tag{5}$$

where U is a non-empty bounded Lebesgue measurable control set defined as

$$U = \{u_i(t) : u_i(t) \in [0,\ 1],\ i = 1, 2, \ldots, 5\}. \tag{6}$$

3.2. Theoretical analysis of the optimal control LF model (3)

3.2.1. Existence of optimal control quintuple

Establishment of the result concerned with the existence of optimal control quintuple necessary for minimizing the objective functional (4) is explored in this section.

Theorem 3.1. *There exists an optimal control quintuple, $u^* = (u_i^*)$, $i = 1, 2, \ldots, 5$, that minimizes the cost functional C in (4), which is defined on the control set U in (6) and constrained by the state system (3) with nonnegative initial conditions $S_{h_1}(0)$, $S_{h_2}(0)$, $I_h(0)$, $T_h(0)$, $R_h(0)$, $S_r(0)$ and $I_r(0)$ when the following properties hold (Asamoah et al., 2022; Fleming and Rishel, 1975):*

(i) The admissible control set U is convex and closed.

(ii) The state system (3) is bounded by a linear function in the state and control variables.

(iii) The integrand of the objective functional C in (4) is convex with respect to the controls.

(iv) There exist constants $\vartheta_1, \vartheta_2 > 0$ and $\vartheta_3 > 1$ such that the Lagrangian is bounded below by

$$\vartheta_1 \left(\sum_{i=1}^{5} |u_i|^2 \right)^{\vartheta_3/2} - \vartheta_2.$$

Proof. Let the control set $U = [0,\ 1]^5$, $u = (u_1, u_2, u_3, u_4, u_5) \in U$, $x = (S_{h_1}, S_{h_2}, I_h, T_h, R_h, S_r, I_r)$ and $F(t, x, u)$, the right-hand side of the state system (3), be expressed as

$$F(t,x,u) = \begin{pmatrix} (1-\sigma)\Lambda_h + \pi\phi_h R_h + u_5(t)S_{h_2} - \epsilon(1-\nu)\Lambda_h I_h - \eta\left(\frac{(1-u_2(t))\beta_h I_h}{1+\alpha_1 I_h} + \frac{(1-u_1(t))\beta_{rh} I_r}{1+\alpha_2 I_r}\right) S_{h_1} - \mu_h S_{h_1} \\ \sigma\Lambda_h + (1-\pi)\phi_h R_h - \epsilon\nu\Lambda_h I_h - \left(\frac{(1-u_2(t))\beta_h I_h}{1+\alpha_1 I_h} + \frac{(1-u_1(t))\beta_{rh} I_r}{1+\alpha_2 I_r}\right) S_{h_2} - \mu_h S_{h_2} - u_5(t)S_{h_2} \\ \left(\frac{(1-u_2(t))\beta_h I_h}{1+\alpha_1 I_h} + \frac{(1-u_1(t))\beta_{rh} I_r}{1+\alpha_2 I_r}\right)(\eta S_{h_1} + S_{h_2}) + \epsilon\Lambda_h I_h - (\alpha_h + \gamma_h + \tau_1 u_3(t) + \mu_h + \delta_h) I_h \\ \alpha_h I_h - \theta\sigma_h T_h - (1-\theta)\delta_h T_h - \mu_h T_h \\ (\gamma_h + \tau_1 u_3(t)) I_h + \theta\sigma_h T_h - (\phi_h + \mu_h) R_h \\ \Lambda_r - \frac{(1-u_1(t))\beta_{hr} S_r I_h}{1+\alpha_1 I_h} - \frac{(1-u_1(t))\beta_r S_r I_r}{1+\alpha_2 I_r} - (\mu_r + \tau_2 u_4(t)) S_r \\ \frac{(1-u_1(t))\beta_{hr} S_r I_h}{1+\alpha_1 I_h} + \frac{(1-u_1(t))\beta_r S_r I_r}{1+\alpha_2 I_r} - (\mu_r + \tau_2 u_4(t)) I_r \end{pmatrix}. \tag{7}$$

Then, it is easy to establish properties (i) to (iv) of Theorem (3.1) above.

(i) By definition of the control set $U = [0,\ 1]^5$, U is closed. In addition, let $y = (y_1, y_2, \ldots, y_5) \in U$ and $z = (z_1, z_2, \ldots, z_5) \in U$ be any two arbitrary points. Then, by the definition of a convex set (Rector et al., 2005),

$$\varphi y_i + (1-\varphi) z_i \in [0,\ 1]^5, \text{ for all } \varphi \in [0,\ 1],\ i = 1, 2, \ldots, 5.$$

So, $\varphi y + (1-\varphi) z \in U$, establishing the convexity of U.

(ii) Following the ideas of previous researchers (Asamoah et al., 2022), and making use of the explicit algorithm presented in Abidemi et al. (2022a), this property is established as follows. Clearly, $F(t, x, u)$ in (7) can be written in the form

$$F(t,x,u) = F_1(t,x) + F_2(t,x)u,$$

where

$$F_1(t,x) = \begin{pmatrix} (1-\sigma)\Lambda_h + \pi\phi_h R_h - \epsilon(1-\nu)\Lambda_h I_h - \left(\mu_h + \frac{\beta_h \eta I_h}{1+\alpha_1 I_h} + \frac{\beta_{rh}\eta I_r}{1+\alpha_2 I_r}\right) S_{h_1} \\ \sigma\Lambda_h + (1-\pi)\phi_h R_h - \epsilon\nu\Lambda_h I_h - \left(\mu_h + \frac{\beta_h I_h}{1+\alpha_1 I_h} + \frac{\beta_{rh} I_r}{1+\alpha_2 I_r}\right) S_{h_2} \\ \left(\frac{\beta_h I_h}{1+\alpha_1 I_h} + \frac{\beta_{rh} I_r}{1+\alpha_2 I_r}\right)(\eta S_{h_1} + S_{h_2}) + \epsilon\Lambda_h I_h - (\alpha_h + \gamma_h + \mu_h + \delta_h) I_h \\ \alpha_h I_h - \theta\sigma_h T_h - (1-\theta)\delta_h T_h - \mu_h T_h \\ \gamma_h I_h + \theta\sigma_h T_h - (\phi_h + \mu_h) R_h \\ \Lambda_r - \frac{\beta_{hr} S_r I_h}{1+\alpha_1 I_h} - \frac{\beta_r S_r I_r}{1+\alpha_2 I_r} - \mu_r S_r \\ \frac{\beta_{hr} S_r I_h}{1+\alpha_1 I_h} + \frac{\beta_r S_r I_r}{1+\alpha_2 I_r} - \mu_r I_r \end{pmatrix}$$

and

$$F_2(t,x) = \begin{pmatrix} \frac{\beta_{rh}\eta S_{h_1} I_r}{1+\alpha_2 I_r} & \frac{\beta_h \eta S_{h_1} I_h}{1+\alpha_1 I_h} & 0 & 0 & S_{h_2} \\ \frac{\beta_{rh} S_{h_2} I_r}{1+\alpha_2 I_r} & \frac{\beta_h S_{h_2} I_h}{1+\alpha_1 I_h} & 0 & 0 & -S_{h_2} \\ -\frac{\beta_{rh}(\eta S_{h_1} + S_{h_2}) I_r}{1+\alpha_2 I_r} & -\frac{\beta_h(\eta S_{h_1} + S_{h_2}) I_h}{1+\alpha_1 I_h} & -\tau_1 I_h & 0 & 0 \\ 0 & 0 & 0 & 0 & 0 \\ 0 & 0 & \tau_1 I_h & 0 & 0 \\ \frac{\beta_{hr} S_r I_h}{1+\alpha_1 I_h} + \frac{\beta_r S_r I_r}{1+\alpha_2 I_r} & 0 & 0 & -\tau_2 S_r & 0 \\ -\frac{\beta_{hr} S_r I_h}{1+\alpha_1 I_h} - \frac{\beta_r S_r I_r}{1+\alpha_2 I_r} & 0 & 0 & -\tau_2 I_r & 0 \end{pmatrix}.$$

Thus,

$$\begin{aligned} \|F(t,x,u)\| &\leq \|F_1(t,x)\| + \|F_2(t,x)\|\|u\| \\ &\leq a_1 + a_2\|u\|, \end{aligned}$$

where $a_1 > 0$ and $a_2 > 0$ are constants determined as

$$a_1 = \sqrt{\max\{b_1, b_2, b_3, b_4, b_5, b_6, b_7\}\left((\Lambda_h\Lambda_r)^2 + \Lambda_h^3\Lambda_r + \Lambda_h\Lambda_r^3 + \Lambda_h^2 + \Lambda_r^2 + \Lambda_h^4 + \Lambda_r^4\right)}$$

and

$$a_2 = \sqrt{\max\{c_1, c_2, c_3, c_4, c_5, c_6\}\left((\Lambda_h\Lambda_r)^2 + \Lambda_h\Lambda_r^3 + \Lambda_h^2 + \Lambda_r^2 + \Lambda_h^4 + \Lambda_r^4\right)},$$

with

$$b_1 = \frac{\beta_{rh}^2(1+\eta)^2}{\mu_h^2(\mu_r + \alpha_2\Lambda_r)^2} + \frac{\beta_{hr}^2}{\mu_r^2(\mu_h + \alpha_1\Lambda_h)^2},$$

$$b_2 = \frac{2\beta_h\beta_{rh}(1+\eta)^2}{\mu_h^2(\mu_h + \alpha_1\Lambda_h)(\mu_r + \alpha_2\Lambda_r)} + \frac{2\beta_{rh}\epsilon(1+\eta)}{\mu_h^2(\mu_r + \alpha_2\Lambda_r)} = \frac{2\beta_{rh}(1+\eta)}{\mu_h^2(\mu_r + \alpha_2\Lambda_r)}\left[\frac{\beta_h(1+\eta)}{(\mu_h + \alpha_1\Lambda_h)} + \epsilon\right],$$

$$b_3 = \frac{2\beta_r\beta_{hr}}{\mu_r^2(\mu_h + \alpha_1\Lambda_h)(\mu_r + \alpha_2\Lambda_r)},$$

$$b_4 = \frac{1}{\mu_h^2}\left[\mu_h^2(1 - 2\sigma + 2\sigma^2) + \alpha_h^2 + \gamma_h^2 + \phi_h^2 - 2\pi(1-\pi)\phi_h^2 + \theta\sigma_h(\theta\sigma_h + 2\gamma_h) + 2\mu_h\phi_h((1-\sigma)\pi + (1-\pi)\sigma)\right],$$

$$b_5 = 1,\ b_6 = \frac{1}{\mu_h^2}\left[\frac{\beta_h(1+\eta)}{(\mu_h + \alpha_1\Lambda_h)}\left(\frac{\beta_h(1+\eta)}{(\mu_h + \alpha_1\Lambda_h)} + 2\epsilon\right) + \epsilon^2\right],\ b_7 = \frac{\beta_r^2}{\mu_r^2(\mu_r + \alpha_2\Lambda_r)^2},$$

$$c_1 = \frac{2\beta_{rh}^2(1 + \eta + \eta^2)}{\mu_h^2(\mu_r + \alpha_2\Lambda_r)^2} + \frac{2\beta_{hr}^2}{\mu_r^2(\mu_h + \alpha_1\Lambda_h)^2},\ c_2 = \frac{4\beta_r\beta_{hr}}{\mu_r^2(\mu_h + \alpha_1\Lambda_h)(\mu_r + \alpha_2\Lambda_r)},\ c_3 = \frac{2(1+\tau_1^2)}{\mu_h^2},$$

$$c_4 = \frac{2\tau_2^2}{\mu_r^2},\ c_5 = \frac{2\beta_h^2(1 + \eta + \eta^2)}{\mu_h^2(\mu_h + \alpha_1\Lambda_h)^2},\ c_6 = \frac{2\beta_r^2}{\mu_r^2(\mu_r + \alpha_2\Lambda_h)^2}.$$

(iii) The integrand of the objective functional C in (4) is the Lagrangian which takes the form

$$\mathcal{L}(t,x,u) = A_1 I_h + A_2(S_r + I_r) + \frac{1}{2}\sum_{i=1}^{5} B_i u_i^2. \tag{8}$$

So, let the two arbitrary points $y, z \in U$ be as previously considered in (i) with $\varphi \in [0,1]$. It is then suffices to show that

$$\mathcal{L}(t,x,(1-\varphi)y + \varphi z) \leq (1-\varphi)\mathcal{L}(t,x,y) + \varphi\mathcal{L}(t,x,z). \tag{9}$$

Now, in view of (8),

$$\mathcal{L}(t,x,(1-\varphi)y + \varphi z) = A_1 I_h + A_2(S_r + I_r) + \frac{1}{2}\sum_{i=1}^{5}\left(B_i((1-\varphi)y_i + \varphi z_i)^2\right) \tag{10}$$

and

$$(1-\varphi)\mathcal{L}(t,x,y) + \varphi\mathcal{L}(t,x,z) = A_1 I_h + A_2(S_r + I_r) + \frac{1}{2}(1-\varphi)\sum_{i=1}^{5} B_i y_i^2 + \frac{1}{2}\varphi\sum_{i=1}^{5} B_i z_i^2. \tag{11}$$

Using inequality (9), the results in (10) and (11) lead to

$$\begin{aligned}\mathcal{L}(t,x,(1-\varphi)y + \varphi z) - ((1-\varphi)\mathcal{L}(t,x,y) + \varphi\mathcal{L}(t,x,z)) &= \frac{1}{2}\varphi(\varphi-1)\sum_{i=1}^{5} B_i(y_i - z_i)^2 \\ &\leq 0, \text{ since } \varphi \in [0,\ 1].\end{aligned}$$

This indicates that the integrand $\mathcal{L}(t,x,u)$ of the objective functional C is convex.

(iv) Recall from (8) that the Lagrangian $\mathcal{L}(t,x,u)$ associated with the objective functional C is given as

$$\begin{aligned}\mathcal{L}(t,x,u) &= A_1 I_h + A_2(S_r + I_r) + \frac{1}{2}\sum_{i=1}^{5} B_i u_i^2 \\ &\geq \frac{1}{2}\sum_{i=1}^{5} B_i u_i^2 \\ &\geq \vartheta_1\left(|u_1|^2 + |u_2|^2 + |u_3|^2 + |u_4|^2 + |u_5|^2\right)^{\vartheta_3/2} - \vartheta_2\end{aligned}$$

where, $\vartheta_1 = 1/2\max\{B_i\},\ i = 1,2,\ldots,5$, $\vartheta_2 > 0$ and $\vartheta_3 = 2$.

□

3.2.2. Characterization of optimal control quintuple

In an attempt to derive the necessary conditions that an optimal control quintuple of the state system (3) must satisfy, PMP by Pontryagin et al. (1962) is made use of. By employing this principle, the optimal control problem involving the cost functional C (4) subject to the state system (3) is converted into a problem of minimizing pointwise a Hamiltonian $\mathcal{H}$ with respect to the control functions u_1, u_2, u_3, u_4 and u_5. The Hamiltonian $\mathcal{H}$ for the optimal control problem is given by

$$\mathcal{H} = \mathcal{L}(t,x,u) + \sum_{j=1}^{7}\lambda_j G_j, \tag{12}$$

where the Lagrangian $\mathcal{L}(t,x,u)$ is as defined in (8), λ_j are the adjoint variables corresponding to the state variables S_{h_1}, S_{h_2}, I_h, T_h, R_h, S_r and I_r, respectively, and G_j is the right-hand side of the non-autonomous system (3) for the j-th state. The characterization result summarized in Theorem 3.2 is claimed for the optimal control problem.

Theorem 3.2. *Given an optimal control quintuple* $u^* = (u_i^*),\ i = 1, 2, \ldots, 5$, *which satisfies* (5), *there exist adjoint variables* $\lambda_j,\ j = 1, 2, \ldots, 7$, *satisfying*

$$
\begin{aligned}
\frac{d\lambda_1}{dt} &= \lambda_1\mu_h + (\lambda_1 - \lambda_3)\eta\left(\frac{(1-u_2)\beta_h I_h}{1+\alpha_1 I_h} + \frac{(1-u_1)\beta_{rh} I_r}{1+\alpha_2 I_r}\right),\\
\frac{d\lambda_2}{dt} &= -\lambda_1 u_5 + \lambda_2(\mu_h + u_5) + (\lambda_2 - \lambda_3)\left[\frac{(1-u_2)\beta_h I_h}{1+\alpha_1 I_h} + \frac{(1-u_1)\beta_{rh} I_r}{1+\alpha_2 I_r}\right],\\
\frac{d\lambda_3}{dt} &= -A_1 + \lambda_1\epsilon(1-\nu)\Lambda_h + \lambda_2\epsilon\nu\Lambda_h - \lambda_3\epsilon\Lambda_h + \lambda_3(\alpha_h + \gamma_h + \tau_1 u_3 + \mu_h + \delta_h)\\
&\quad + (\lambda_1 - \lambda_3)\frac{(1-u_2)\beta_h\eta S_{h_1}}{1+\alpha_1 I_h} + (\lambda_3 - \lambda_1)\frac{(1-u_2)\beta_h\eta\alpha_1 S_{h_1} I_h}{(1+\alpha_1 I_h)^2}\\
&\quad + (\lambda_2 - \lambda_3)\frac{(1-u_2)\beta_h S_{h_2}}{1+\alpha_1 I_h} + (\lambda_3 - \lambda_2)\frac{(1-u_2)\beta_h\alpha_1 S_{h_2} I_h}{(1+\alpha_1 I_h)^2}\\
&\quad - \lambda_4\alpha_h - \lambda_5(\gamma_h + \tau_1 u_3) + (\lambda_6 - \lambda_7)\frac{(1-u_1)\beta_{hr} S_r}{1+\alpha_1 I_h} + (\lambda_7 - \lambda_6)\frac{(1-u_1)\beta_{hr}\alpha_1 S_r I_h}{(1+\alpha_1 I_h)^2},\\
\frac{d\lambda_4}{dt} &= \lambda_4(\theta\sigma_h + (1-\theta)\delta_h + \mu_h) - \lambda_5\theta\sigma_h,\\
\frac{d\lambda_5}{dt} &= -\lambda_1\pi\phi_h - \lambda_2(1-\pi)\phi_h + \lambda_5(\phi_h + \mu_h),\\
\frac{d\lambda_6}{dt} &= -A_2 + \lambda_6(\mu_r + \tau_2 u_4) + (\lambda_6 - \lambda_7)(1-u_1)\left(\frac{\beta_{hr} I_h}{1+\alpha_1 I_h} + \frac{\beta_r I_r}{1+\alpha_2 I_r}\right),\\
\frac{d\lambda_7}{dt} &= -A_2 + (\lambda_1 - \lambda_3)\frac{(1-u_1)\beta_{rh}\eta S_{h_1}}{1+\alpha_2 I_r} + (\lambda_3 - \lambda_1)\frac{(1-u_1)\beta_{rh}\eta\alpha_2 S_{h_1} I_r}{(1+\alpha_2 I_r)^2}\\
&\quad + (\lambda_2 - \lambda_3)\frac{(1-u_1)\beta_{rh} S_{h_2}}{1+\alpha_2 I_r} + (\lambda_3 - \lambda_2)\frac{(1-u_1)\beta_{rh}\alpha_2 S_{h_2} I_r}{(1+\alpha_2 I_r)^2}\\
&\quad + \lambda_7(\mu_r + \tau_2 u_4) + (\lambda_6 - \lambda_7)\frac{(1-u_1)\beta_r S_r}{1+\alpha_2 I_r} + (\lambda_7 - \lambda_6)\frac{(1-u_1)\beta_r\alpha_2 S_r I_r}{(1+\alpha_2 I_r)^2},
\end{aligned}
\tag{13}
$$

with the terminal conditions

$$
\lambda_j(t_f) = 0 \quad (\textit{where } j = 1, 2, \ldots, 7) \tag{14}
$$

and control characterizations

$$
\begin{aligned}
u_1^* &= \min\left\{\max\left\{0, \frac{(\lambda_3 - \lambda_1)\beta_{rh}\eta S_{h_1} I_r(1+\alpha_1 I_h) + (\lambda_3 - \lambda_2)\beta_{rh} S_{h_2} I_r(1+\alpha_1 I_h) + Q}{B_1(1+\alpha_1 I_h)(1+\alpha_2 I_r)}\right\}, 1\right\},\\
u_2^* &= \min\left\{\max\left\{0, \frac{(\lambda_3 - \lambda_1)\beta_h\eta S_{h_1} I_h + (\lambda_3 - \lambda_2)\beta_h S_{h_2} I_h}{B_2(1+\alpha_1 I_h)}\right\}, 1\right\},\\
u_3^* &= \min\left\{\max\left\{0, \frac{(\lambda_3 - \lambda_5)\tau_1 I_h}{B_3}\right\}, 1\right\},\\
u_4^* &= \min\left\{\max\left\{0, \frac{(\lambda_6 S_r + \lambda_7 I_r)\tau_2}{B_4}\right\}, 1\right\},\\
u_5^* &= \min\left\{\max\left\{0, \frac{(\lambda_2 - \lambda_1) S_{h_2}}{B_5}\right\}, 1\right\},
\end{aligned}
\tag{15}
$$

where $Q = (\lambda_7 - \lambda_6)[\beta_{hr} S_r I_h(1+\alpha_2 I_r) + \beta_r S_r I_r(1+\alpha_1 I_h)]$.

Proof. The Hamiltonian $\mathcal{H}$ in (12) can be written in its explicit form as

$$\begin{aligned}
\mathcal{H} &= A_1 I_h + A_2(S_r + I_r) + \frac{1}{2}\left(B_1 u_1^2 + B_2 u_2^2 + B_3 u_3^2 + B_4 u_4^2 + B_5 u_5^2\right) \\
&+ \lambda_1 \left\{ (1-\sigma)\Lambda_h + \pi\phi_h R_h + u_5(t) S_{h_2} - \epsilon(1-\nu)\Lambda_h I_h - \eta\left(\frac{(1-u_2(t))\beta_h I_h}{1+\alpha_1 I_h} + \frac{(1-u_1(t))\beta_{rh} I_r}{1+\alpha_2 I_r}\right) S_{h_1} - \mu_h S_{h_1} \right\} \\
&+ \lambda_2 \left\{ \sigma\Lambda_h + (1-\pi)\phi_h R_h - \epsilon\nu\Lambda_h I_h - \left(\frac{(1-u_2(t))\beta_h I_h}{1+\alpha_1 I_h} + \frac{(1-u_1(t))\beta_{rh} I_r}{1+\alpha_2 I_r}\right) S_{h_2} - \mu_h S_{h_2} - u_5(t) S_{h_2} \right\} \\
&+ \lambda_3 \left\{ \left(\frac{(1-u_2(t))\beta_h I_h}{1+\alpha_1 I_h} + \frac{(1-u_1(t))\beta_{rh} I_r}{1+\alpha_2 I_r}\right)(\eta S_{h_1} + S_{h_2}) + \epsilon\Lambda_h I_h - (\alpha_h + \gamma_h + \tau_1 u_3(t) + \mu_h + \delta_h) I_h \right\} \\
&+ \lambda_4 \left\{ \alpha_h I_h - \theta\sigma_h T_h - (1-\theta)\delta_h T_h - \mu_h T_h \right\} \\
&+ \lambda_5 \left\{ (\gamma_h + \tau_1 u_3(t)) I_h + \theta\sigma_h T_h - (\phi_h + \mu_h) R_h \right\} \\
&+ \lambda_6 \left\{ \Lambda_r - \frac{(1-u_1(t))\beta_{hr} S_r I_h}{1+\alpha_1 I_h} - \frac{(1-u_1(t))\beta_r S_r I_r}{1+\alpha_2 I_r} - (\mu_r + \tau_2 u_4(t)) S_r \right\} \\
&+ \lambda_7 \left\{ \frac{(1-u_1(t))\beta_{hr} S_r I_h}{1+\alpha_1 I_h} + \frac{(1-u_1(t))\beta_r S_r I_r}{1+\alpha_2 I_r} - (\mu_r + \tau_2 u_4(t)) I_r \right\}.
\end{aligned}$$

Then, it is straightforward to derive the adjoint system (13) from

$$-\frac{d\lambda_j}{dt} = \frac{\partial \mathcal{H}}{\partial x}, \qquad \lambda_i(t_f) = 0,$$

where $j = 1, 2, \ldots, 7$ and $x = S_{h_1}, S_{h_2}, I_h, T_h, R_h, S_r, I_r$. Further, the optimal control quintuple $u_i^*,\ i = 1, 2, \ldots, 5$, are derived by solving

$$\frac{\partial \mathcal{H}}{\partial u_i} = 0 \text{ for } u_i^*,\ i = 1, 2, \ldots, 5,$$

so that

$$\begin{aligned}
&B_1 u_1^* - \frac{(\lambda_3 - \lambda_1)\beta_{rh}\eta S_{h_1} I_r(1+\alpha_1 I_h) + (\lambda_3 - \lambda_2)\beta_{rh} S_{h_2} I_r(1+\alpha_1 I_h) + Q}{(1+\alpha_1 I_h)(1+\alpha_2 I_r)} = 0, \\
&B_2 u_2^* - \frac{(\lambda_3 - \lambda_1)\beta_h \eta S_{h_1} I_h + (\lambda_3 - \lambda_2)\beta_h S_{h_2} I_h}{1+\alpha_1 I_h} = 0, \\
&B_3 u_3^* - (\lambda_3 - \lambda_5)\tau_1 I_h = 0, \\
&B_4 u_4^* - (\lambda_6 S_r + \lambda_7 I_r)\tau_2 = 0, \\
&B_5 u_5^* - (\lambda_2 - \lambda_1) S_{h_2} = 0,
\end{aligned} \tag{16}$$

where $Q = (\lambda_7 - \lambda_6)[\beta_{hr} S_r I_h(1+\alpha_2 I_r) + \beta_r S_r I_r(1+\alpha_1 I_h)]$. Hence, it follows from (16) that

$$\begin{aligned}
&u_1^* = \frac{(\lambda_3 - \lambda_1)\beta_{rh}\eta S_{h_1} I_r(1+\alpha_1 I_h) + (\lambda_3 - \lambda_2)\beta_{rh} S_{h_2} I_r(1+\alpha_1 I_h) + Q}{B_1(1+\alpha_1 I_h)(1+\alpha_2 I_r)}, \\
&u_2^* = \frac{(\lambda_3 - \lambda_1)\beta_h \eta S_{h_1} I_h + (\lambda_3 - \lambda_2)\beta_h S_{h_2} I_h}{B_2(1+\alpha_1 I_h)},\ u_3^* = \frac{(\lambda_3 - \lambda_5)\tau_1 I_h}{B_3}, \\
&u_4^* = \frac{(\lambda_6 S_r + \lambda_7 I_r)\tau_2}{B_4},\ u_5^* = \frac{(\lambda_2 - \lambda_1) S_{h_2}}{B_5}.
\end{aligned} \tag{17}$$

Finally, imposition of the bounds $0 \le u_i \le 1,\ i = 1, 2, \ldots, 5$, on the results derived in (17) leads to arriving at the control characterization in (15). □

Furthermore, by standard arguments, the control characterization (15) can be expressed in a piecewise form as

$$u_i^* = \begin{cases} 0 & \text{if } \varpi_i^* \le 0 \\ \varpi_i^* & \text{if } 0 \le \varpi_i \le 1, \\ 1 & \text{if } \varpi_i^* \ge 1, \end{cases}$$

where $i = 1, 2, \ldots, 5$ and with

$$\varpi_1^* = \frac{(\lambda_3 - \lambda_1)\beta_{rh}\eta S_{h_1} I_r(1 + \alpha_1 I_h) + (\lambda_3 - \lambda_2)\beta_{rh} S_{h_2} I_r(1 + \alpha_1 I_h) + Q}{B_1(1 + \alpha_1 I_h)(1 + \alpha_2 I_r)},$$
$$\varpi_2^* = \frac{(\lambda_3 - \lambda_1)\beta_h \eta S_{h_1} I_h + (\lambda_3 - \lambda_2)\beta_h S_{h_2} I_h}{B_2(1 + \alpha_1 I_h)},\ \varpi_3^* = \frac{(\lambda_3 - \lambda_5)\tau_1 I_h}{B_3},$$
$$\varpi_4^* = \frac{(\lambda_6 S_r + \lambda_7 I_r)\tau_2}{B_4},\ \varpi_5^* = \frac{(\lambda_2 - \lambda_1) S_{h_2}}{B_5}.$$

4. Numerical simulations, and efficiency and cost-effectiveness analyses

4.1. Numerical simulations

Due to different time horizons for the state system's initial conditions and the adjoint system's terminal conditions (14), the widely used Runge-Kutta-based forward-backward sweep method in literature (Falowo et al., 2022; Asamoah et al., 2022) is employed for solving the optimality system numerically. The optimality system of 14-dimensional system of ODEs consists of the non-autonomous system (3) and adjoint system (13) coupled with the control characterization (15). The numerical experiments are carried out using MATLAB with the guide of procedure for forward-backward sweep method outlined by Lenhart and Workman in Lenhart and Workman (2007).

For the simulations, initial conditions for the states are taken from Abidemi et al. (2022b) as $S_{h_1}(0) = 137252$, $S_{h_2}(0) = 68627$, $I_h(0) = 124$, $T_h(0) = 79$, $R_h(0) = 58$, $S_r(0) = 2060160$, and $I_r(0) = 1240$, while the numerical values of the model parameters are as presented in Table 2. In addition, τ_1 is assumed to be 0.35 while τ_2 is fixed at $\tau_2 = 0.75$ (Peter et al., 2020). The numerical values of the weight constants in the cost functional C (4) are chosen as $A_1 = 1$, $A_2 = 1$, $B_1 = 0.010$, $B_2 = 0.010$, $B_3 = 0.010$, $B_4 = 0.010$, $B_5 = 0.010$. The simulations are conducted over the time horizon $t \in [0,\ t_f]$, where the final duration of controls implementation $t_f = 50$ days. It is worthy of noting that all the weight values considered in the simulations are theoretical as they are used only for illustrations of the control interventions proposed by this study.

Table 2: Parameters of model (1) with their numerical values (Abidemi et al., 2022b)

Parameter	Value	Parameter	Value
Λ_h	0.01	α_1	0.65
Λ_r	0.00001	α_2	0.65
η	0.65	θ	0.612
β_h	0.0844	ν	0.5
β_{hr}	0.0844	α_h	0.2148541
β_{rh}	0.0372	σ	0.5
β_r	0.0372	σ_h	0.0123
ϵ	0.015	γ_h	0.433
μ_h	0.0003	μ_r	0.0627
δ_h	0.0001923	ϕ_h	0.7354
ψ_h	0.2985	π	0.5

To optimize the objective functional (4), implementation of different set of control combination strategies ranging from single to quintuple control interventions are considered.

4.1.1. Single control implementation

To be specific, the set of single interventions consists of five different control strategies, namely, environmental fumigation with pesticide ($u_1(t)$) only, use of condom ($u_2(t)$) only, use of antiviral therapy ($u_3(t)$) only, rodent reduction control ($u_4(t)$) only and educational campaign ($u_5(t)$) only.

4.1.2. Double control implementation

To optimize the objective functional (4) with the efforts of double control interventions, five different combination strategies of two out of the five optimal controls $u_i(t)$, $i = 1, 2, \ldots, 5$, are considered in this paper. These are combination of environmental fumigation ($u_1(t)$) and use of condom ($u_2(t)$) only, combination of environmental fumigation ($u_1(t)$) and rodent reduction control ($u_4(t)$) only, combination of condom usage ($u_2(t)$) and use of antiviral therapy ($u_3(t)$) only, combination of condom usage ($u_2(t)$) and rodent reduction control ($u_4(t)$) only and combination of use of antiviral therapy ($u_3(t)$) and educational campaign ($u_5(t)$) only.

4.1.3. Triple control implementation

For triple control intervention, we are particular about five optimal control combination strategies defined as follows: Combination of environmental fumigation with pesticide ($u_1(t)$), use of condom ($u_2(t)$) and rodent reduction control ($u_4(t)$) only, combination of environmental fumigation ($u_1(t)$), use of antiviral therapy ($u_3(t)$) and educational campaign ($u_5(t)$) only, combination of environmental fumigation ($u_1(t)$), rodent reduction control ($u_4(t)$) and educational campaign ($u_5(t)$) only, combination of use of condom ($u_2(t)$), use of antiviral therapy ($u_3(t)$) and rodent reduction control ($u_4(t)$) only and combination of use of antiviral therapy ($u_3(t)$), rodent reduction control ($u_4(t)$) and educational campaign ($u_5(t)$) only.

4.1.4. Quadruple control implementation

Here, quadruple control intervention is implemented by specifically consider the following five optimal control combination strategies: Combination of environmental fumigation with pesticide ($u_1(t)$), use of condom ($u_2(t)$), use of antiviral therapy ($u_3(t)$) and rodent reduction control ($u_4(t)$) only, combination of environmental fumigation ($u_1(t)$), use of condom ($u_2(t)$), use of antiviral therapy ($u_3(t)$) and educational campaign ($u_5(t)$) only, combination of environmental fumigation ($u_1(t)$), use of condom ($u_2(t)$), rodent reduction control ($u_4(t)$) and educational campaign ($u_5(t)$) only, combination of environmental fumigation ($u_1(t)$), use of antiviral therapy ($u_3(t)$), rodent reduction control ($u_4(t)$) and educational campaign policy ($u_5(t)$) only and combination of condom usage ($u_2(t)$), use of antiviral therapy ($u_3(t)$), rodent reduction control ($u_4(t)$) and educational campaign ($u_5(t)$) only.

4.1.5. Quintuple control implementation

Quintuple control intervention is a single optimal control strategy which combines all the five control interventions, namely, environmental fumigation with pesticide ($u_1(t)$), use of condom ($u_2(t)$), use of antiviral therapy ($u_3(t)$), rodent reduction control ($u_4(t)$) and educational campaign ($u_5(t)$). This control intervention is considered

as part of the implemented control interventions investigated in this work with a view to effectively optimize the objective functional (4).

4.2. Efficiency and cost-effectiveness analysis

In economic evaluation of an intervention strategy, efficiency and cost-effectiveness are two different important keys in prioritizing the implementation of a particular intervention from the set of competing and alternative strategies in disease control.

On one hand, efficiency analysis (EA) helps to identify the intervention that prevents the highest number of infections in human population with no regard to the cost of control implementation (Ghosh et al., 2019). According to this analysis, an intervention with the highest efficiency index (EI) is most efficient (Abidemi and Aziz, 2022; Falowo et al., 2022). On the other hand, cost-effectiveness analysis (CEA) helps in determining the intervention strategy that averts infection mostly at the least possible cost Falowo et al. (2022). Following the ideas of authors in some previous works (Abidemi and Aziz, 2022; Falowo et al., 2022), EI is simply given as

$$\text{EI} = \frac{\text{Total infection averted by intervention}}{\text{Total infection without intervention}} \times 100. \tag{18}$$

In carrying out the cost-effectiveness analysis, the incremental cost-effectiveness ratio (ICER) is often adopted. This cost analysis method has been applied to determine the most cost-effective intervention in the control of diseases by a number of researchers (Asamoah et al., 2020, 2022; Cantor and Ganiats, 1999; Ojo et al., 2022; Omame et al., 2021). ICER measures the ratio between costs and health benefits of any two interventions competing for the same limited resources. The calculation of ICER makes use of the following formula:

$$\text{ICER} = \frac{\Delta \text{ in total costs of interventions}}{\Delta \text{ in total infection averted by interventions}}. \tag{19}$$

5. Results

5.1. Numerical results of the optimal control LF model (3)

Figure 1 shows how the objective functional C (4) is optimized when any of the single control interventions is implemented. The numerical solutions of the optimal control variables $u_i(t)$, $i = 1, 2, \ldots, 5$, associated with the implementation of single control interventions are displayed in Fig. 2.

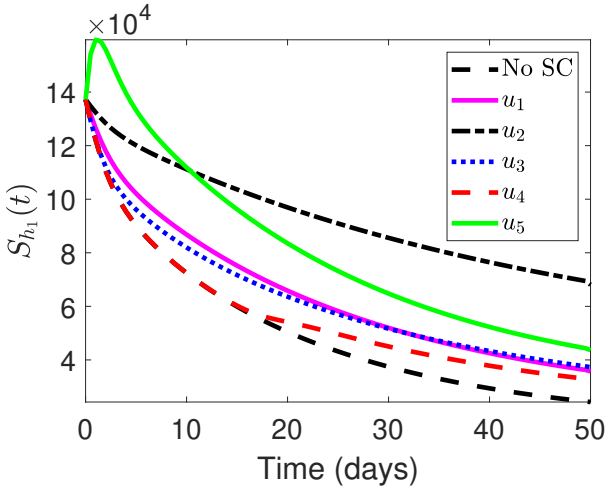

(a) Dynamics of S_{h_1}

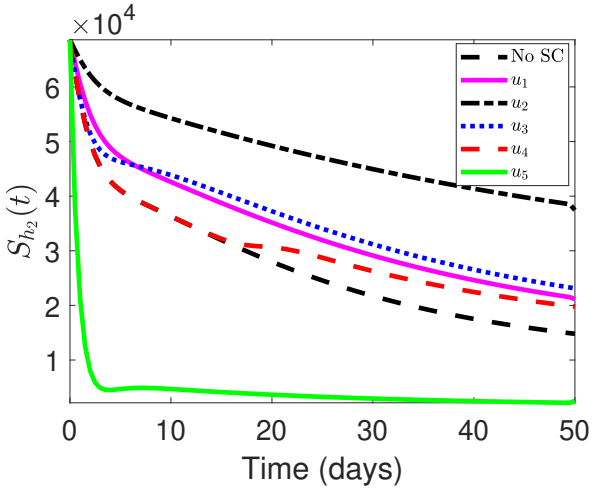

(b) Dynamics of S_{h_2}

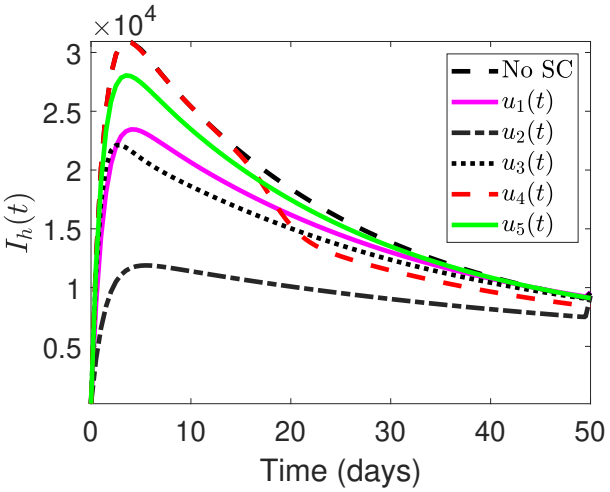

(c) Dynamics of I_h

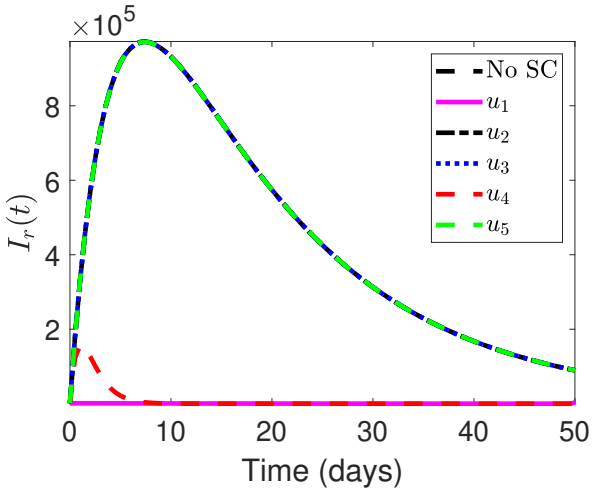

(d) Dynamics of I_r

Fig. 1: Effects of single control (SC) implementation on the dynamics of model (3)

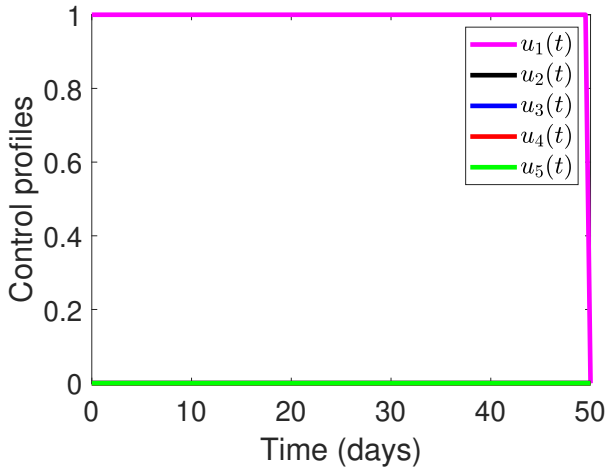

(a)

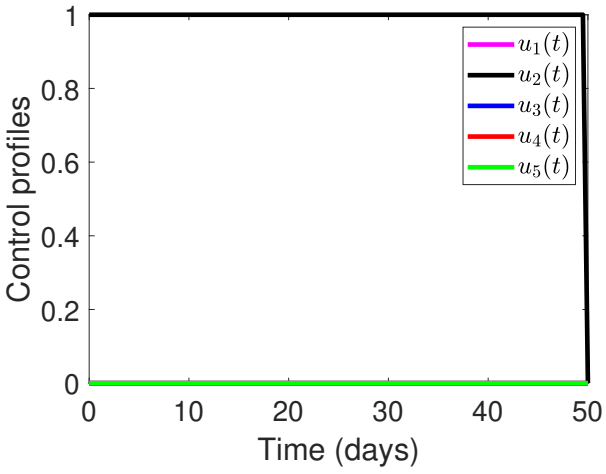

(b)

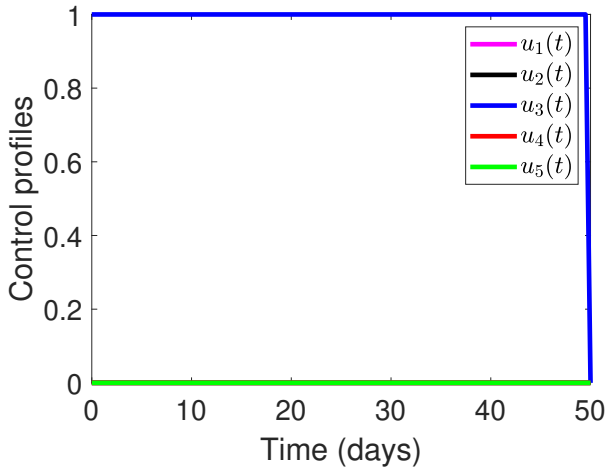

(c)

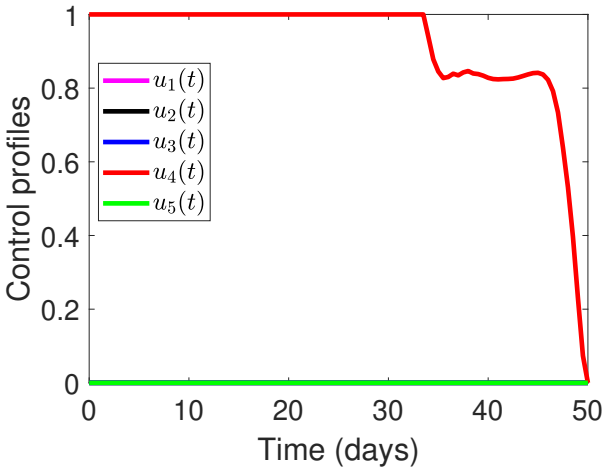

(d)

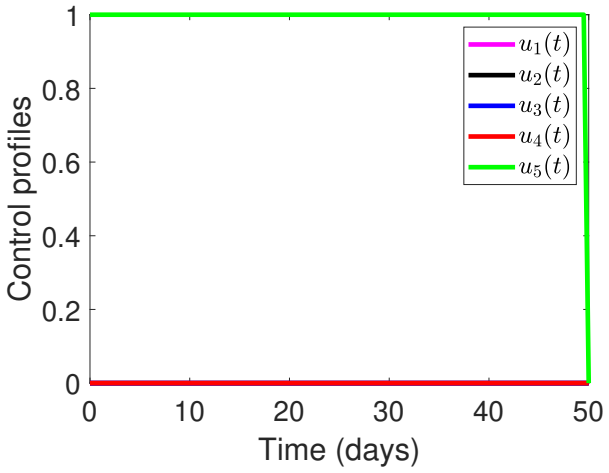

(e)

Fig. 2: Single control (SC) profiles of the LF model (3)

In Fig. 3, the time series plots of the simulations of optimal control LF model (3) which show the comparisons of application of five different combinations of two of the five optimal control variables and when no intervention is put in place are demonstrated, while Fig. 4 displays the control profiles for the implementation of these double interventions.

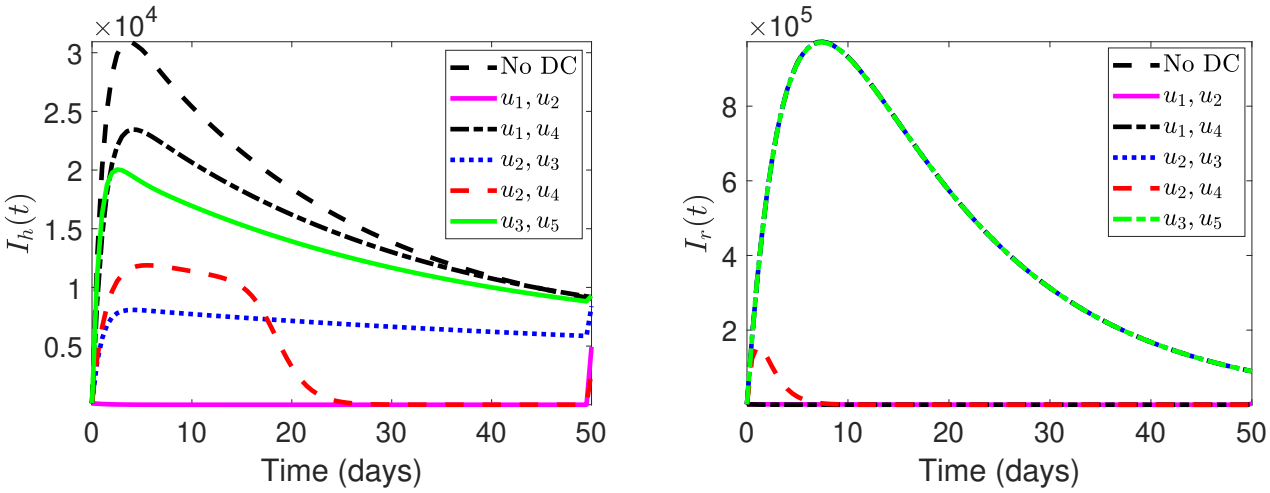

(a) Dynamics of I_h

(b) Dynamics of I_r

Fig. 3: Effects of double control (DC) implementation on the dynamics of model (3)

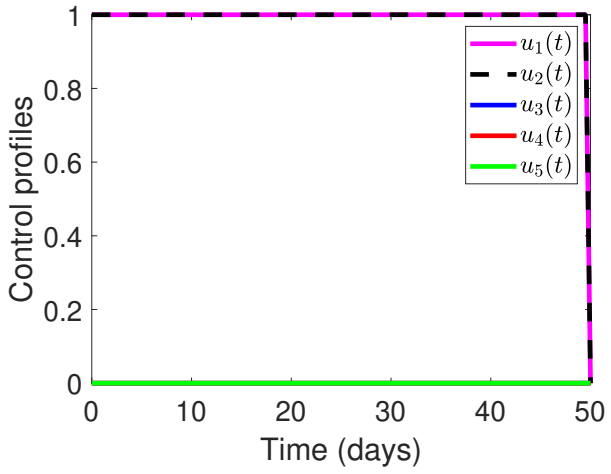

(a)

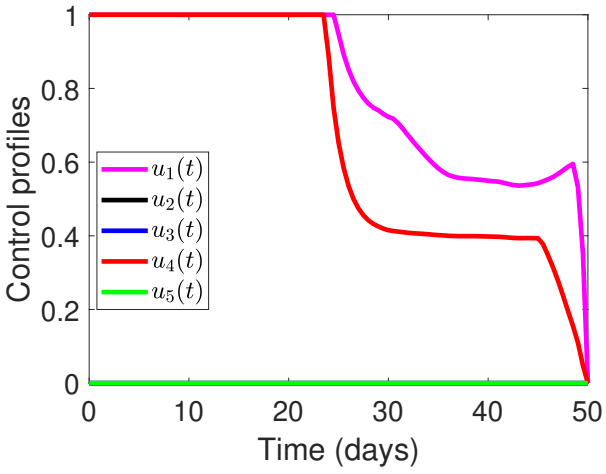

(b)

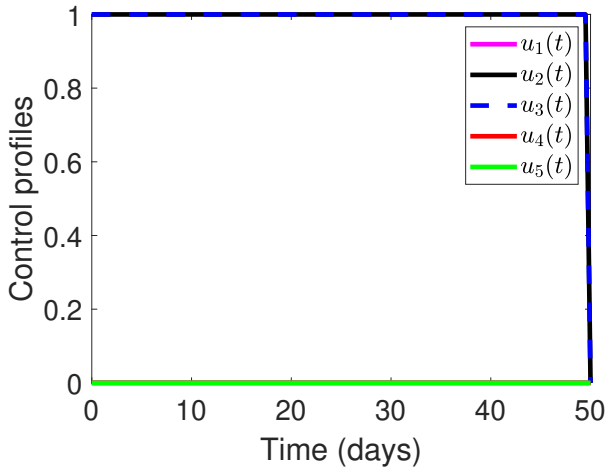

(c)

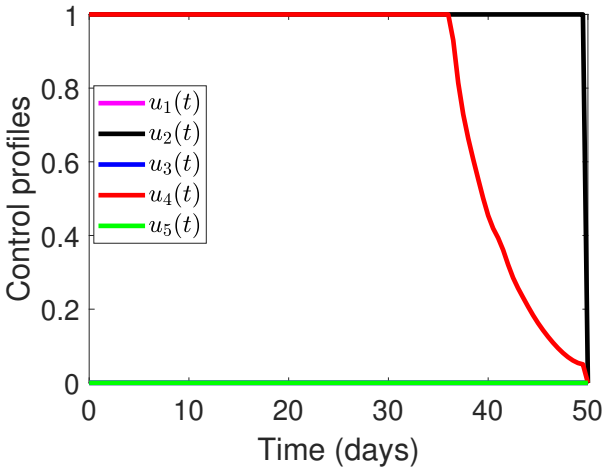

(d)

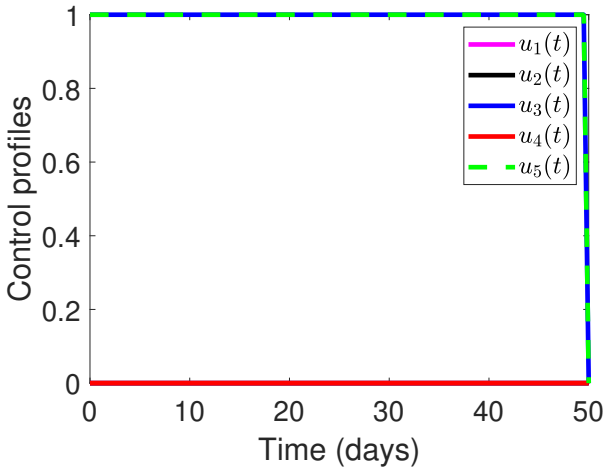

(e)

Fig. 4: Double control (DC) profiles of the LF model (3)

Furthermore, the time series plots of the simulations of optimal control LF model (3) which reveal the comparisons of the implementation of combinations of three out of the five control variables with no control intervention at the human and rodent populations level are displayed in Fig. 5. The numerical solutions of the time-dependent control variables for the triple interventions are graphically illustrated in Fig. 6.

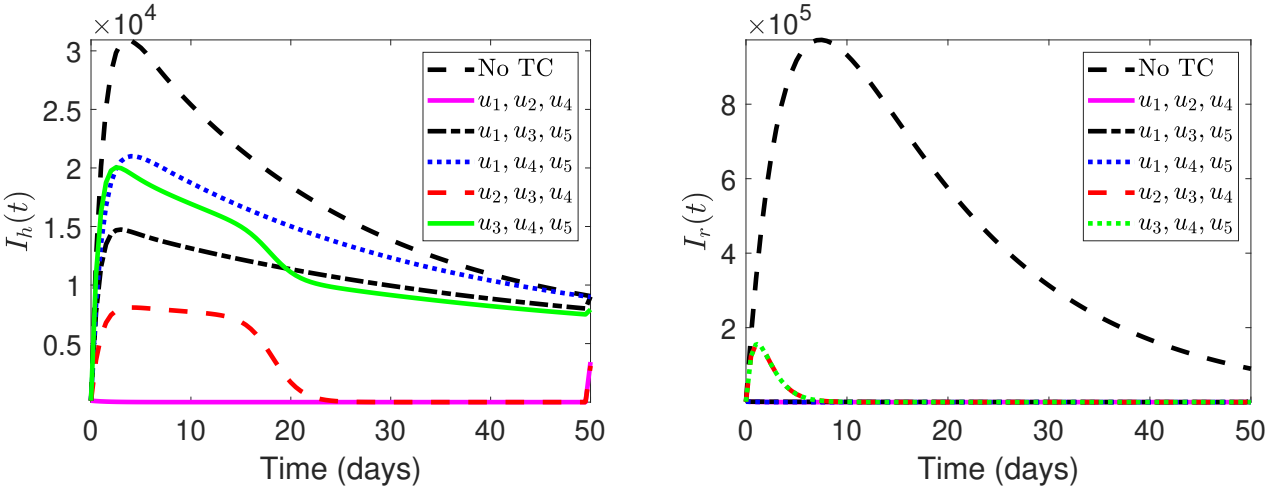

(a) Dynamics of I_h

(b) Dynamics of I_r

Fig. 5: Effects of triple control (TC) implementation on the dynamics of model (3)

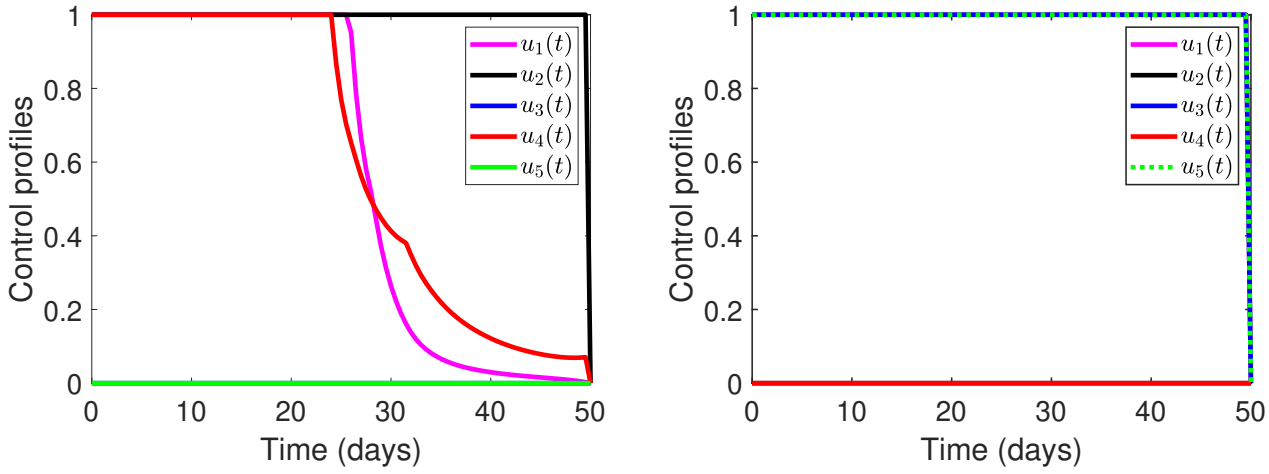

(a)

(b)

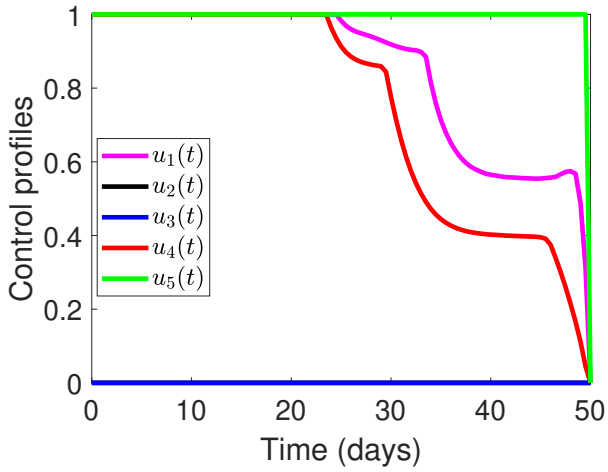

(c)

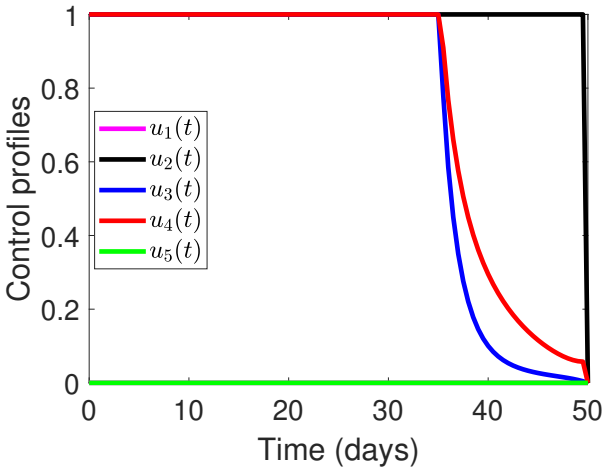

(d)

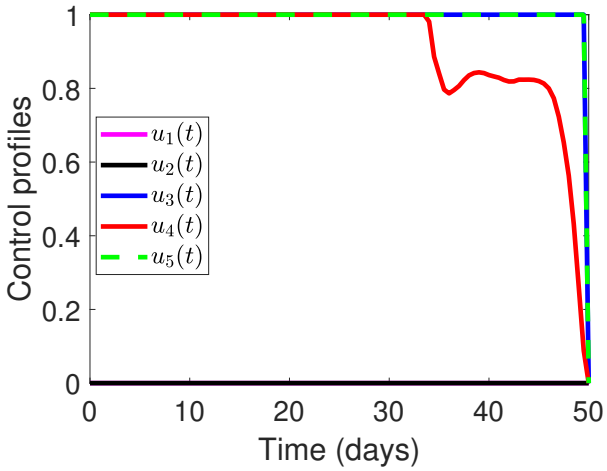

(e)

Fig. 6: Triple control (TC) profiles of the LF model (3)

Comparisons of the impacts of five different combinations of four out of the five control variables and when no any effort of control implementation is put in place on the dynamics of LF between the interacting populations of human and rodent are assessed through the numerical simulation of the optimal control LF model (3) as presented by the time series plots in Fig. 7. The corresponding profiles for the control solutions for different combinations of four of the given five control variables $u_i(t)$, $i = 1, 2, \ldots, 5$, necessary for minimizing the objective functional (4) are presented in Fig. 8.

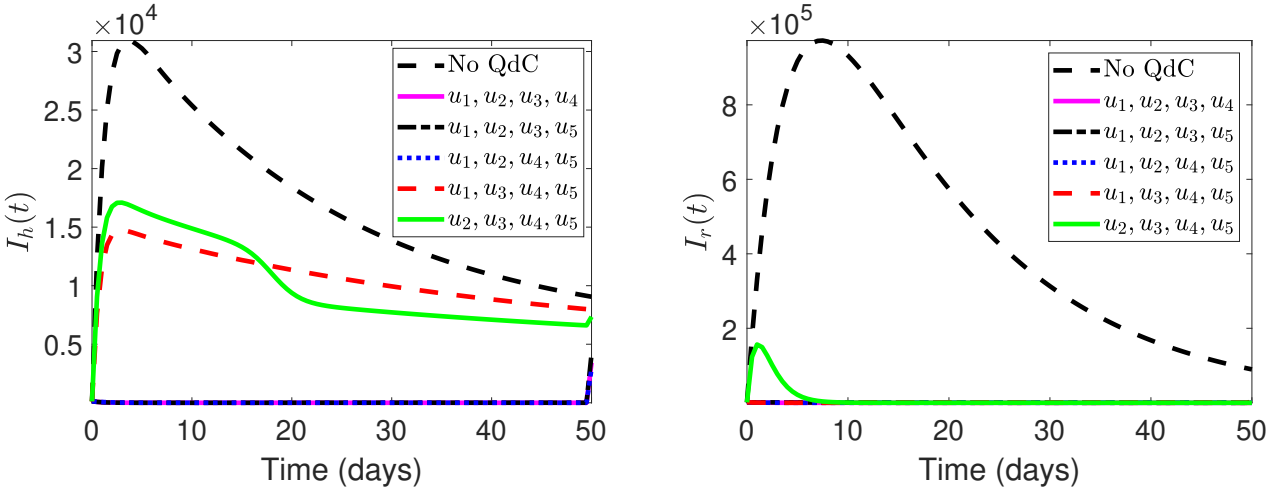

(a) Dynamics of I_h

(b) Dynamics of I_r

Fig. 7: Effects of quadruple control (QdC) implementation on the dynamics of model (3)

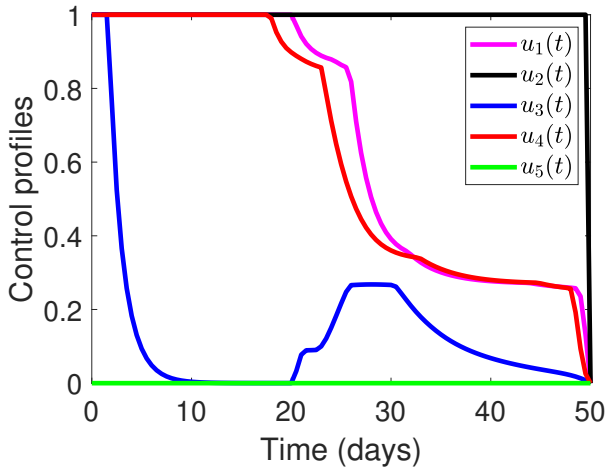

(a)

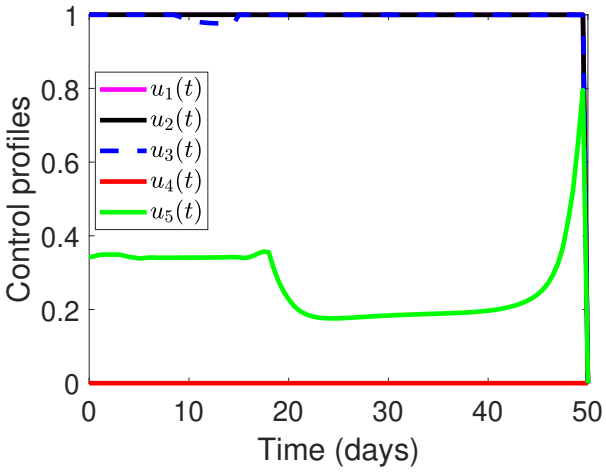

(b)

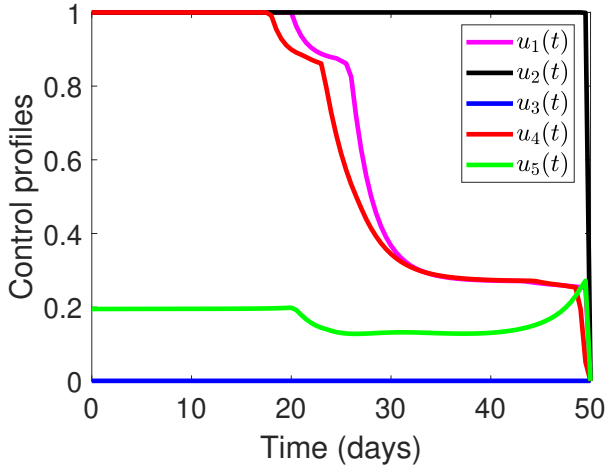

(c)

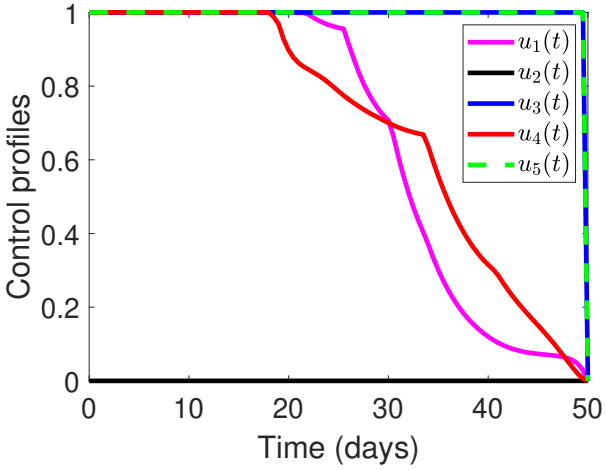

(d)

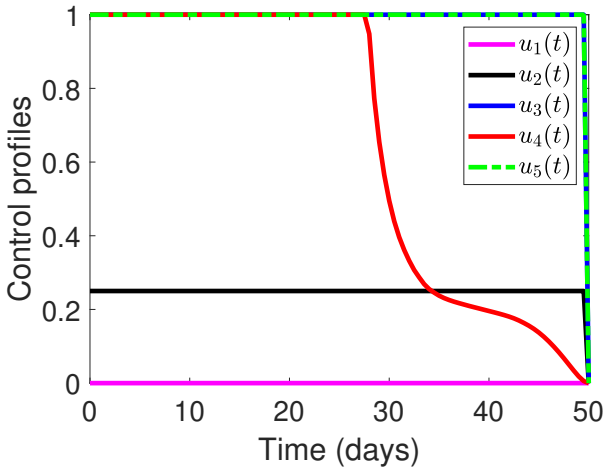

(e)

Fig. 8: Quadruple control (QdC) profiles of the LF model (3)

Figure 9 shows how the optimal control LF model (3) behaves when the combination of all the five optimal controls $u_i(t)$, $i = 1, 2, \ldots, 5$, is implemented and the solutions of the optimal control variables associated with the intervention strategy.

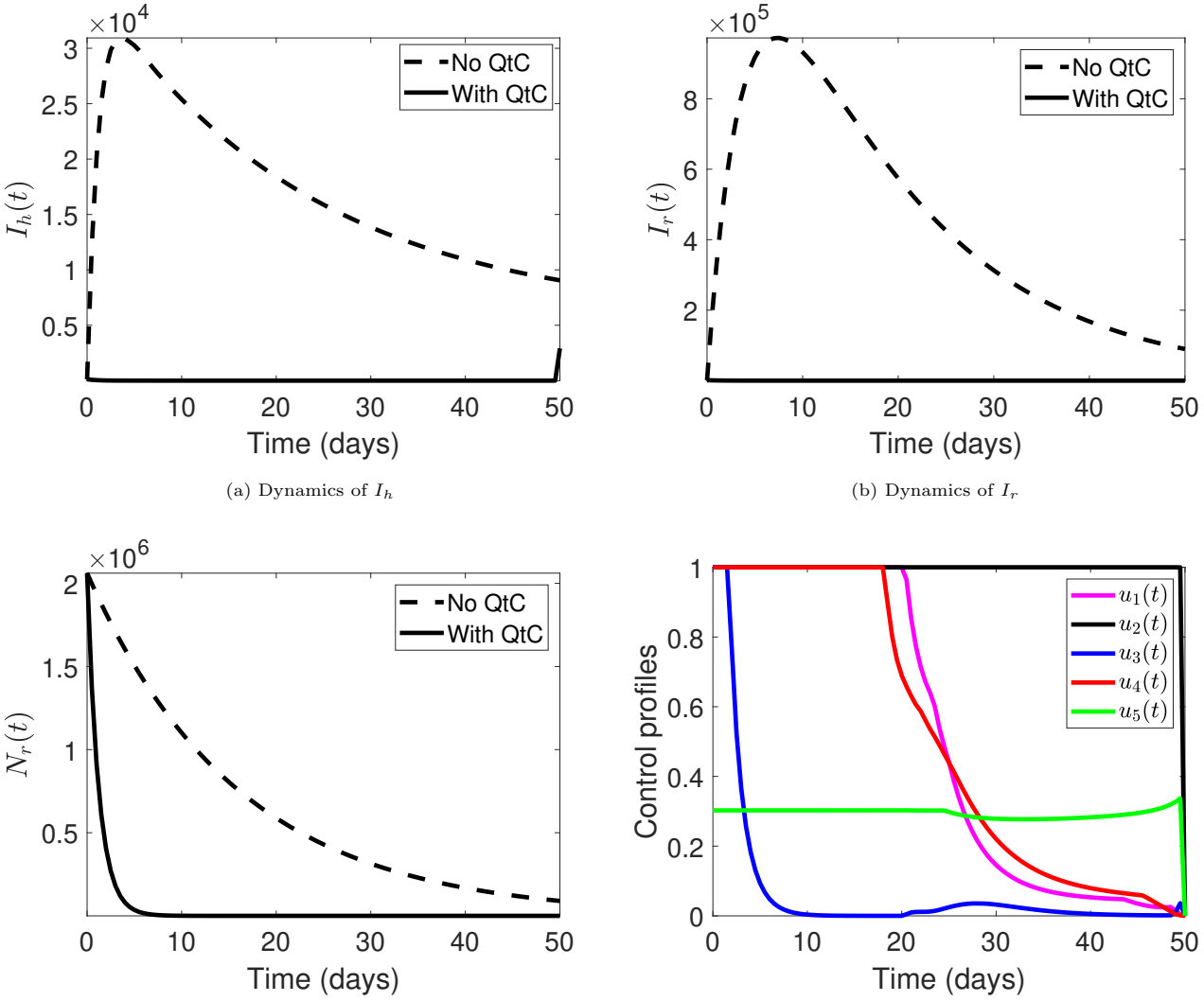

(a) Dynamics of I_h

(b) Dynamics of I_r

(c) Dynamics of N_r

(d) Quintuple control (QtC) profiles

Fig. 9: Effects of quintuple control (QtC) implementation on the dynamics of model (3)

5.2. Results of the efficiency and cost-effectiveness analyses

5.2.1. The most efficient and cost-effective single control

In view of the results arising from the implementation of single control interventions on the optimality system, as illustrated in Figs. 1 and 2, EA and CEA are carried out on the single interventions $u_i(t)$, $i = 1, 2, \ldots, 5$. In Table 3, the EI and ICER for individual single interventions arranged from the least to the highest total number of infection averted are shown. As observed from Table 3, intervention $u_2(t)$, denoting condom use, has the highest EI of 45.374%. This is followed by intervention $u_3(t)$ representing antiviral drug therapy, with EI of 18.024%.

The next intervention with highest EI is $u_1(t)$, denoting environmental fumigation, with EI of 13.158% followed by intervention $u_4(t)$, representing rodent reduction control, having EI of 7.749%, while intervention $u_5(t)$ representing educational campaign has the least EI of 5.110%. Thus, intervention $u_2(t)$ representing condom use is the most efficient single control intervention strategy.

Table 3: EI and ICER for single control interventions

Intervention	Total infection averted	Total cost expended on the intervention	Efficiency (%)	ICER ($\times 10^{-4}$)
u_5	8.8535×10^4	49.994	5.110	5.6468
u_4	1.3426×10^5	43.852	7.749	-1.3432
u_1	2.2798×10^5	0.500	13.158	-4.6257
u_3	3.1228×10^5	49.994	18.024	5.8712
u_2	7.8614×10^5	0.500	45.374	-1.0445

In CEA, the dominance of one over the other of any two competing interventions for the same limited resources implies the greater effectiveness at cheaper cost (Cantor and Ganiats, 1999). On this note, an intervention that is being dominated is excluded from the list, while an intervention that dominates in terms of cost effectiveness is retained.

Now, making use of the formula in (19), the ICER is calculated for each of the five single interventions $u_i(t),\ i = 1, 2, \ldots, 5$. For the competing interventions $u_5(t)$ with $u_4(t)$, there is a cost saving of 0.00013432 for intervention $u_4(t)$ over intervention $u_5(t)$. This follows the comparison of ICER values for the two control interventions, which reveals that the ICER value for intervention $u_4(t)$ is less than that of intervention $u_5(t)$ (as Table 3 shows). The lower ICER value for intervention $u_4(t)$ suggests that intervention $u_5(t)$ is strongly dominated by intervention $u_4(t)$. Consequently, intervention $u_5(t)$ representing educational campaign is eliminated from the list. Intervention $u_4(t)$ is further compared with intervention $u_1(t)$. The calculated ICER values for the two intervention strategies in view of formula (19) are summarized in Table 4.

Table 4: ICER for single control interventions excluding u_5

Intervention	Total infection averted	Total cost expended on the intervention	ICER ($\times 10^{-4}$)
u_4	1.3426×10^5	43.852	3.2662
u_1	2.2798×10^5	0.500	-4.6257
u_3	3.1228×10^5	49.994	5.8712
u_2	7.8614×10^5	0.500	-1.0445

As Table 4 shows, the ICER value for intervention $u_4(t)$ is higher than that of intervention $u_1(t)$, implying that intervention $u_1(t)$ strongly dominates intervention $u_4(t)$. Thus, intervention $u_4(t)$ is removed from the list of interventions and alternative control interventions to implement. So, intervention $u_1(t)$ is further compared with intervention $u_3(t)$. In view of formula (19), the computed ICER values for the two competing control interventions

are as displayed in Table 5.

Table 5: ICER for single control interventions further excluding u_4

Intervention	Total infection averted	Total cost expended on the intervention	ICER
u_1	2.2798×10^5	0.500	2.1932×10^{-6}
u_3	3.1228×10^5	49.994	5.8712×10^{-4}
u_2	7.8614×10^5	0.500	-1.0445×10^{-4}

As shown in Table 5, the ICER value for intervention $u_3(t)$ is higher than that of intervention $u_1(t)$, suggesting that intervention $u_3(t)$ is strongly dominated by intervention $u_1(t)$. Hence, intervention $u_3(t)$ is discarded from the set of control interventions. Now, we are left with comparing intervention $u_1(t)$ with intervention $u_2(t)$. At this juncture, it is needless to recalculate ICER further since it can be observed that the same cost is expended on both interventions $u_1(t)$ and $u_2(t)$. However, intervention $u_2(t)$ averts higher number of infection compared to intervention $u_1(t)$. Therefore, intervention $u_2(t)$ representing the use of condom is considered the most cost-effective among the five single interventions examined in this paper. We therefore conclude that condom use intervention $u_2(t)$ is considered the most efficient and most cost-effective single intervention among the five single optimal control interventions under consideration.

5.2.2. The most efficient and cost-effective double control

Table 6 presents the EI and ICER values of different optimal control combination strategies of two of the five control variables. The interventions are arranged in an increasing order with respect to the averted infection. A look at Table 6 shows that the double intervention u_1, u_2 produces 99.689 efficiency, positioning the intervention the most efficient double intervention.

Furthermore, the ICER for each of the interventions is calculated using the formula (19). The results obtained from the calculations are shown in Table 6.

Table 6: EI and ICER for double control interventions

Intervention	Total infection averted	Total cost expended on the intervention ($)	Efficiency (%)	ICER
u_1, u_4	2.2854×10^5	0.637	13.191	2.7873×10^{-6}
u_3, u_5	4.0996×10^5	1.000	23.662	2.0009×10^{-6}
u_2, u_3	1.0453×10^6	1.000	60.330	–
u_2, u_4	1.3294×10^6	0.888	76.728	-3.9423×10^{-7}
u_1, u_2	1.7272×10^6	1.000	99.689	2.8155×10^{-7}

It is seen from Table 6 that the ICER value for the double intervention u_1, u_4 is higher when compared with intervention u_3, u_5. This suggests that intervention u_1, u_4 is strongly dominated. Hence, the double intervention u_1, u_4 is discarded from the list. The double intervention u_3, u_5 is further compared with intervention u_2, u_3. The

computed ICER values using (19) are given in Table 7. The same cost of \$1.00 is expended on both the double

Table 7: ICER for double control interventions excluding intervention u_1, u_4

Intervention	Total infection averted	Total cost expended on the intervention (\$)	ICER
u_3, u_5	4.0996×10^5	1.000	–
u_2, u_3	1.0453×10^6	1.000	–
u_2, u_4	1.3294×10^6	0.888	-3.9423×10^{-7}
u_1, u_2	1.7272×10^6	1.000	2.8155×10^{-7}

interventions u_3, u_5 and u_2, u_3 as Table 7 shows. However, the intervention u_2, u_3 averts higher infection compared to intervention u_3, u_5. Thus, the double intervention u_3, u_5 is eliminated from the list. Then, intervention u_2, u_3 is further compared with intervention u_2, u_4. Using the formula (19), Table 8 presents the summary of computed ICER values. A look at Table 8 indicates that the ICER value for double intervention u_2, u_4 is lower that of

Table 8: ICER for double control interventions further excluding intervention u_3, u_5

Intervention	Total infection averted	Total cost expended on the intervention (\$)	ICER
u_2, u_3	1.0453×10^6	1.000	9.5666×10^{-7}
u_2, u_4	1.3294×10^6	0.888	-3.9423×10^{-7}
u_1, u_2	1.7272×10^6	1.000	2.8155×10^{-7}

intervention u_2, u_3, implying that the double intervention u_2, u_4 strongly dominates the double intervention u_2, u_3. This means that the double intervention u_2, u_3 is more costly to implement. Therefore, double intervention u_2, u_3 is discarded from the list. Finally, double intervention u_2, u_4 is compared with double intervention u_1, u_2. Table 9 provides the calculated ICER values based on formula (19). It is observed from Table 9 that the ICER value

Table 9: ICER for double control interventions further excluding intervention u_2, u_3

Intervention	Total infection averted	Total cost expended on the intervention (\$)	ICER
u_2, u_4	1.3294×10^6	0.888	6.6797×10^{-7}
u_1, u_2	1.7272×10^6	1.000	2.8155×10^{-7}

for intervention u_2, u_4 is higher than the ICER value of intervention u_1, u_2, suggesting that double intervention u_2, u_4 is strongly dominated by intervention u_1, u_2. Consequently, double intervention u_2, u_4 is removed from the list. Therefore, when the available resources are limited, double intervention u_1, u_2 is the most cost-effective intervention among the five different combinations of two controls analysed in this paper. This leads us to arriving at the double intervention u_1, u_2 regarded the most efficient and most cost-effective double intervention of all the five double interventions considered.

5.2.3. The most efficient and cost-effective triple control

Using the simulated results arising from the implementation of five different combination strategies of three of the five control variables (see Fig. 5), Table 10 presents the EI and ICER values for the triple interventions ranked in an increasing order of infection averted. From Table 10, it is seen that combination of the control variables

Table 10: EI and ICER for triple control interventions

Intervention	Total infection averted	Total cost expended on the intervention ($)	Efficiency (%)	ICER
u_1, u_4, u_5	3.3200×10^5	1.209	19.162	3.6416×10^{-6}
u_3, u_4, u_5	5.5861×10^5	1.437	32.242	1.0061×10^{-6}
u_1, u_3, u_5	6.5215×10^5	1.500	37.640	6.7351×10^{-7}
u_2, u_3, u_4	1.4581×10^6	1.235	84.158	-3.2880×10^{-7}
u_1, u_2, u_4	1.7287×10^6	1.050	99.777	-6.8367×10^{-7}

u_1, u_2 and u_4 produces the most efficient triple intervention with efficiency of 99.777%. To ascertain the most cost-effective triple intervention, the ICER values for the five different combination strategies consisting of three of the five control variables are calculated using formula (19). By comparing the ICER for triple intervention u_1, u_4, u_5 and u_3, u_4, u_5, the ICER value for intervention u_3, u_4, u_5 is lower when compared with the ICER for intervention u_1, u_4, u_5, implying that intervention u_3, u_4, u_5 strongly dominates intervention u_1, u_4, u_5. This means that triple intervention u_1, u_4, u_5 is more costly to implement, and therefore discarded from the list. Based on formula (19), the ICER is recalculated for the rest of triple interventions. See Table 11 for the summary of the results. As shown

Table 11: ICER for triple control interventions excluding intervention u_1, u_4, u_5

Intervention	Total infection averted	Total cost expended on the intervention ($)	ICER
u_3, u_4, u_5	5.5861×10^5	1.437	2.5725×10^{-6}
u_1, u_3, u_5	6.5215×10^5	1.500	6.7351×10^{-7}
u_2, u_3, u_4	1.4581×10^6	1.235	-3.2880×10^{-7}
u_1, u_2, u_4	1.7287×10^6	1.050	-6.8367×10^{-7}

in Table 11, the ICER value for intervention u_3, u_4, u_5 is higher than the ICER value for intervention u_1, u_3, u_5. Therefore, intervention u_3, u_4, u_5 is eliminated from the list to preserve the available limited resources. The ICER is further recalculated for the remaining triple control interventions and their ICER values are displayed in Table 12. As Table 12 shows, the ICER value for intervention u_1, u_3, u_5 is higher than that of intervention u_2, u_3, u_4. This implies that intervention u_1, u_3, u_5 is strongly dominated by intervention u_2, u_3, u_4. Therefore, intervention u_1, u_3, u_5 is discarded from the list to preserve the available limited resources. Lastly, the ICER is recalculated for the rest of the two competing triple interventions with their ICER values presented in Table 13. Following the comparison of the ICER values for interventions u_2, u_3, u_4 and u_1, u_2, u_4, it is observed that the ICER value for intervention u_2, u_3, u_4 is higher than the ICER for intervention u_1, u_2, u_4. This simply suggests that intervention

Table 12: ICER for triple control interventions further excluding intervention u_3, u_4, u_5

Intervention	Total infection averted	Total cost expended on the intervention ($)	ICER
u_1, u_3, u_5	6.5215×10^5	1.500	2.3001×10^{-6}
u_2, u_3, u_4	1.4581×10^6	1.235	-3.2880×10^{-7}
u_1, u_2, u_4	1.7287×10^6	1.050	-6.8367×10^{-7}

Table 13: ICER for triple control interventions further excluding intervention u_1, u_3, u_5

Intervention	Total infection averted	Total cost expended on the intervention ($)	ICER
u_2, u_3, u_4	1.4581×10^6	1.235	8.4699×10^{-7}
u_1, u_2, u_4	1.7287×10^6	1.050	-6.8367×10^{-7}

u_1, u_2, u_4 strongly dominates intervention u_2, u_3, u_4. Thus, intervention u_1, u_2, u_4 is cheaper to implement than intervention u_2, u_3, u_4. Therefore, intervention u_1, u_2, u_4 is the most cost-effective triple intervention of the five triple interventions analysed in this paper. As a result, intervention u_1, u_2, u_4 is considered the most efficient and cost-effective triple intervention among the five triple interventions examined.

5.2.4. The most efficient and cost-effective quadruple control

Using the simulation results obtained from the implementation of quadruple interventions on the optimality system as shown in Fig. 7, we further examine the most efficient and most cost-effective intervention from the implemented five different quadruple interventions. The EI and ICER values for the quadruple interventions ranked from least to highest in respect of the infection averted are displayed in Table 14 A look at Table 14 reveals that

Table 14: EI and ICER for quadruple control interventions

Intervention	Total infection averted	Total cost expended on the intervention ($)	Efficiency (%)	ICER
u_1, u_3, u_4, u_5	6.5270×10^5	560.23	37.672	8.5833×10^{-4}
u_2, u_3, u_4, u_5	7.1926×10^5	530.68	41.514	-4.4396×10^{-4}
u_1, u_2, u_3, u_5	1.7277×10^6	51.024	99.719	-4.7564×10^{-4}
u_1, u_2, u_3, u_4	1.7288×10^6	86.918	99.783	0.0326
u_1, u_2, u_4, u_5	1.7292×10^6	54.341	99.805	-0.0814

combination of controls u_1, u_2, u_4, u_5 produces the most efficient quadruple intervention with 99.805% efficiency. In addition, the ICER values for the five quadruple interventions are calculated using formula (19) (see the results in Table 14). Comparing the ICER values for quadruple intervention u_1, u_3, u_4, u_5 and u_2, u_3, u_4, u_5 reveals that the ICER value for intervention u_2, u_3, u_4, u_5 is lower than the ICER value for u_1, u_3, u_4, u_5. Thus, quadruple intervention u_1, u_3, u_4, u_5 is left out, and the ICER is recalculated for the rest of quadruple interventions. Table 15

gives the summary of the results. From Table 15, it is observed that the ICER for intervention u_2, u_3, u_4, u_5 is higher

Table 15: ICER for triple control interventions excluding intervention u_1, u_3, u_4, u_5

Intervention	Total infection averted	Total cost expended on the intervention ($)	ICER
u_2, u_3, u_4, u_5	7.1926×10^5	530.68	7.3781×10^{-4}
u_1, u_2, u_3, u_5	1.7277×10^6	51.024	-4.7564×10^{-4}
u_1, u_2, u_3, u_4	1.7288×10^6	86.918	0.0326
u_1, u_2, u_4, u_5	1.7292×10^6	54.341	-0.0814

when compared with intervention u_1, u_2, u_3, u_5. This simply means that intervention u_1, u_2, u_3, u_5 is less costly to implement than intervention u_2, u_3, u_4, u_5. Thus, intervention u_2, u_3, u_4, u_5 is removed from the list and ICER is recalculated for the rest of quadruple interventions. The results obtained from the computation are presented in Table 16 From Table 16, it is shown that intervention u_1, u_2, u_3, u_4 strongly dominated by intervention u_1, u_2, u_3, u_5

Table 16: ICER for triple control interventions further excluding intervention u_2, u_3, u_4, u_5

Intervention	Total infection averted	Total cost expended on the intervention ($)	ICER
u_1, u_2, u_3, u_5	1.7277×10^6	51.024	2.9533×10^{-5}
u_1, u_2, u_3, u_4	1.7288×10^6	86.918	0.0326
u_1, u_2, u_4, u_5	1.7292×10^6	54.341	-0.0814

as the ICER value for the former is higher than that of the latter. Therefore, intervention u_1, u_2, u_3, u_4 is eliminated from the list, and the rest two competing quadruple interventions are re-examined by calculating their ICER values. See the summary of the results arising from the calculation in Table 17. The ICER value for intervention

Table 17: ICER for triple control interventions further excluding intervention u_1, u_2, u_3, u_4

Intervention	Total infection averted	Total cost expended on the intervention ($)	ICER
u_1, u_2, u_3, u_5	1.7277×10^6	51.024	0.000029533
u_1, u_2, u_4, u_5	1.7292×10^6	54.341	0.0022

u_1, u_2, u_3, u_5 is lower compared to the ICER value of intervention u_1, u_2, u_4, u_5 (as Table 17 shows), implying that intervention u_1, u_2, u_3, u_5 strongly dominates intervention u_1, u_2, u_4, u_5. Hence, intervention u_1, u_2, u_4, u_5 is left out to preserve the limited resources. Therefore, from the above analysis, quadruple intervention u_1, u_2, u_3, u_5 is the most cost-effective among the five possible combinations of four control variables in case of limited available resources. Whereas quadruple intervention u_1, u_2, u_4, u_5 is the most efficient intervention to be implemented when no attention is paid to the cost of control implementation.

5.2.5. Efficiency of quintuple control

In light of the results graphically illustrated in Fig. 9, the efficiency of the quintuple intervention is 99.813%, which led to the intervention averting the highest number of symptomatic infections in humans with 1.7293×10^6 (see Table 18) when compared with all other possible combinations analysed in this paper.

Table 18: EI for quintuple control intervention

Intervention	Total infection averted	Total cost expended on the intervention ($)	Efficiency (%)
u_1, u_2, u_3, u_4, u_5	1.7293×10^6	71.536	99.813

5.2.6. Determination of the overall most cost-effective control intervention

Apart from determining the most cost-effective single, double, triple, quadruple and quintuple interventions among the various interventions in the same categories, it is also desirable to ascertain the overall most cost-effective intervention to be implemented. In this regard, all the single, double, triple, quadruple and quintuple interventions considered the most cost-effective are re-examined by calculating ICER for them. The interventions are ranked in ascending order according to the total infection averted as Table 19 shows.

Table 19: ICER for the most cost-effective single, double, triple, quadruple and quintuple interventions

Intervention	Total infection averted	Total cost expended on the intervention ($)	ICER
u_2	7.8614×10^5	0.500	6.3602×10^{-7}
u_1, u_2	1.7272×10^6	1.000	5.3132×10^{-7}
u_1, u_2, u_3, u_5	1.7277×10^6	51.024	0.1000
u_1, u_2, u_4	1.7287×10^6	1.050	-0.0500
u_1, u_2, u_3, u_4, u_5	1.7293×10^6	71.536	0.1175

Comparing the single intervention u_2 and double intervention u_1, u_2, it is shown that the ICER value for former is higher than that of latter. Thus, the single intervention u_2 is left out, and the rest of interventions are re-examined. The results of computations are presented in Table 20.

Table 20: ICER for the most cost-effective double, triple, quadruple and quintuple interventions

Intervention	Total infection averted	Total cost expended on the intervention ($)	ICER
u_1, u_2	1.7272×10^6	1.000	5.7897×10^{-7}
u_1, u_2, u_3, u_5	1.7277×10^6	51.024	0.1000
u_1, u_2, u_4	1.7287×10^6	1.050	-0.0500
u_1, u_2, u_3, u_4, u_5	1.7293×10^6	71.536	0.1175

From Table 20, comparison of double intervention u_1, u_2 and quadruple intervention u_1, u_2, u_3, u_5 reveals that the ICER of intervention u_1, u_2 is lower than the ICER of u_1, u_2, u_3, u_5. This simply implies that quadruple intervention u_1, u_2, u_3, u_5 is strongly dominated by double intervention u_1, u_2. Therefore, quadruple intervention u_1, u_2, u_3, u_5 is discarded from the list to preserve the limited resources. Further computations are carried out for the rest of competing interventions as Table 21 displays. Comparing the double intervention u_1, u_2 and triple

Table 21: ICER for the most cost-effective double, triple and quintuple interventions

Intervention	Total infection averted	Total cost expended on the intervention ($)	ICER
u_1, u_2	1.7272×10^6	1.000	5.7897×10^{-7}
u_1, u_2, u_4	1.7287×10^6	1.050	3.3333×10^{-5}
u_1, u_2, u_3, u_4, u_5	1.7293×10^6	71.536	0.1175

intervention u_1, u_2, u_4, the triple intervention u_1, u_2, u_4 is discarded and the remaining two competing intervention are re-examined as shown in Table 22.

Table 22: ICER for the most cost-effective double and quintuple interventions

Intervention	Total infection averted	Total cost expended on the intervention ($)	ICER
u_1, u_2	1.7272×10^6	1.000	5.7897×10^{-7}
u_1, u_2, u_3, u_4, u_5	1.7293×10^6	71.536	3.3589×10^{-2}

Table 22 shows that the ICER of quintuple intervention u_1, u_2, u_3, u_4, u_5 is higher when compared with the ICER of double intervention u_1, u_2. This means that double intervention u_1, u_2 strongly dominates quintuple intervention u_1, u_2, u_3, u_4, u_5, implying that the quintuple intervention is more costly to implement. Therefore, quintuple intervention u_1, u_2, u_3, u_4, u_5 is left out to preserve the limited resources. Therefore, double intervention u_1, u_2 is the overall most cost-effective intervention of all the possible combinations of optimal controls u_1, u_2, u_3, u_4 and u_5 analysed in this paper.

6. Discussion of results

Under Sect. 5, five different single control interventions are implemented. It is noticed from Fig. 1(c) that the population of infected individuals with control is mostly reduced with the implementation of single intervention $u_2(t)$, followed by interventions $u_3(t)$, $u_1(t)$, $u_4(t)$ and $u_5(t)$, respectively, when compared with the population without any single control intervention. Figure 1(d) shows that the number of infected rodents diminishes when either of single interventions $u_1(t)$ or $u_4(t)$ is put in place, whereas implementation of the three other single interventions ($u_2(t)$, $u_3(t)$ and $u_5(t)$) makes no significant impact in the reduction of infected rodent population size. Furthermore, the use of intervention $u_5(t)$ led to most of the susceptible individuals with poor community hygiene improving their community hygiene over the duration of control implementation as Figs. 1(a) and 1(b) show. To achieve the

optimal solutions illustrated by Fig. 1, each of environmental fumigation $u_1(t)$, condom use $u_2(t)$, antiviral drug therapy $u_3(t)$ and educational campaign $u_5(t)$ is to be fully implemented for about 49 days before reducing sharply to the minimum level in final time of implementation (see Figs. 2(a) to 2(c) and Fig. 2(e), respectively), while rodent reduction control $u_4(t)$ should be implemented at 100% maximum level in the first 33 days of implementation period before dropping gradually to the minimum level over the remaining control implementation time horizon $t \in (34,\ 50]$ (in days) as shown in Fig. 2(d).

By implementing the various double control interventions under consideration, it is noticed from Fig. 3(a) that subpopulation of infectious individuals with double control intervention mostly reduced with combination of $u_1(t)$ and $u_2(t)$, followed by combinations of $u_2(t)$ and $u_4(t)$, $u_2(t)$ and $u_3(t)$, $u_3(t)$ and u_5, and $u_1(t)$ and $u_4(t)$ compared to the subpopulation without any intervention. Moreover, the subpopulation of infectious rodent diminishes with combinations of $u_1(t)$ and $u_2(t)$, $u_1(t)$ and $u_4(t)$, and $u_2(t)$ and $u_4(t)$, whereas the interventions combining $u_2(t)$ and $u_3(t)$, and $u_3(t)$ and u_5 do not affect the dynamic of the subpopulation significantly as shown in Fig. 3(b). Control profiles for the double interventions are displayed in Fig. 4. It is seen that the combination of $u_1(t)$ and $u_2(t)$ will optimize the objective functional (4) if the both controls are sustained at maximum level of implementation for about 49 days before dropping to the minimum level in the final time as Fig. 4(a) shows. Similar observations are made for double interventions $u_2(t)$ and $u_3(t)$ (see Fig. 4(c)) and $u_3(t)$ and $u_5(t)$ (see Fig. 4(e)). Further, the combination $u_1(t)$ and $u_4(t)$ requires the maximal use of $u_1(t)$ and $u_4(t)$ in the first 25 days and 23 days, respectively, before reducing gradually to the minimum level in the final time of control implementation to optimally minimize the objective functional (4) as seen in Fig. 4(b). Figure 4(d) suggests that, to minimize the objective functional (4) with combination $u_2(t)$ and $u_4(t)$, control $u_2(t)$ should be held maximally for almost the implementation period, while control $u_4(t)$ should be maintained at maximal level for 36 days before decreasing gradually to the minimal level at final time.

With application of triple control interventions, it is observed that combination $u_1(t)$, $u_2(t)$ and $u_4(t)$ most positively impacts the dynamics of symptomatic infectious subpopulation. See Fig. 5(a). This is followed by combination $u_2(t)$, $u_3(t)$ and $u_4(t)$, combination $u_1(t)$, $u_3(t)$ and $u_5(t)$ and combination $u_3(t)$, $u_4(t)$ and $u_5(t)$. The subpopulation is least affected positively by combination $u_1(t)$, $u_4(t)$ and $u_5(t)$. In addition, all the five triple interventions are sufficient to diminish the total number of infectious rodents in the rodent population as depicted in Fig. 5(b). To achieve the optimal solutions illustrated in Fig. 5, Fig. 6 describes how the combinations of three of the given five control variables should be optimally used over the implementation period. It is noticed that the combination of $u_1(t)$, $u_2(t)$ and $u_4(t)$ will optimize the objective functional (4) if control $u_2(t)$ is implemented maximally for almost full period, while the controls $u_1(t)$ and $u_4(t)$ are maintained at upper bound for 25 days and 23 days, respectively, before reducing gradually to the lower bound in final time as shown in Fig. 6(a). For combination $u_1(t)$, $u_3(t)$ and $u_5(t)$, Fig. 6(b) suggests that it requires all the three controls to be maximally used for 49 days before dropping sharply to the minimum level in final time. From Fig. 6(c), it is observed that combination $u_1(t)$, $u_4(t)$ and $u_5(t)$ requires maximal use of control $u_5(t)$ for almost implementation period while controls $u_1(t)$ and $u_2(t)$ need to be maintained at maximum level for about 25 days and 23 days, respectively. Combination $u_2(t)$, $u_3(t)$ and $u_4(t)$ requires maximal use of $u_2(t)$ for almost full period with maximal use of controls $u_3(t)$ and $u_4(t)$ for 35 days before reducing to zero use (see Fig. 6(d)). As shown in Fig. 6(e), combination $u_3(t)$, $u_4(t)$ and $u_5(t)$

requires maximal use of controls $u_3(t)$ and $u_5(t)$ for almost full implementation period (49 days) and maximal use of control $u_4(t)$ for about 33 days before decreasing gradually to zero use in final time.

Similarly, quadruple control interventions are implemented in order to optimize the objective functional (4). From Fig. 7, it is seen that combination $u_1(t)$, $u_2(t)$, $u_4(t)$ and $u_5(t)$ most positively impacts the dynamics of symptomatic infectious subpopulation (see Fig. 7(a)). The next most positively impactful combination is $u_1(t)$, $u_2(t)$, $u_3(t)$ and $u_4(t)$, followed by combination $u_1(t)$, $u_2(t)$, $u_3(t)$ and $u_5(t)$, combination $u_2(t)$, $u_3(t)$, $u_4(t)$ and $u_5(t)$ then combination $u_1(t)$, $u_3(t)$, $u_4(t)$ and $u_5(t)$. Further, it is noticed that all the five quadruple interventions are sufficient to diminish the total number of infectious rodents when implemented (as Fig. 7(b) reveals). To achieve these optimal solutions, combination $u_1(t)$, $u_2(t)$, $u_3(t)$ and $u_4(t)$ requires the controls to be maximally implemented for about 23 days, 49 days, 3 days and 20 days, respectively (as shown in Fig. 8(a)). For combination $u_1(t)$, $u_2(t)$, $u_3(t)$ and $u_5(t)$, maximal use of controls $u_1(t)$, $u_2(t)$ and $u_3(t)$ is required for almost full implementation period, while control $u_5(t)$ starts at a rate of about 0.34 (34%) and slowly increase to a maximum of about 0.80 (80%) (as Fig. 8(b) displays). Combination $u_1(t)$, $u_2(t)$, $u_4(t)$ and $u_5(t)$ requires maximal use of controls $u_1(t)$, $u_2(t)$ and $u_4(t)$ for about 23 days, 49 days and 20 days, respectively, while control $u_5(t)$ starts at about 0.2 (20%) and slowly increase to a maximum of about 0.3 (30%) as observed from Fig. 8(c). Combination $u_1(t)$, $u_3(t)$, $u_4(t)$ and $u_5(t)$ will minimize the objective functional (4) if the controls are used maximally for 22 days, 49 days, 16 days and 49 days, respectively (see Fig. 8(d)). It is noticed that combination $u_2(t), u_3(t), u_4(t), u_5(t)$ requires maximal use of controls $u_3(t)$, $u_4(t)$ and $u_5(t)$ for 49 days, 27 days and 49 days, respectively, while control $u_2(t)$ is constantly held at a maximal level of about 0.25 (25%) for almost full period of implementation (see Fig. 8(e)).

Noticeably, application of quintuple control intervention (combined effort of all the controls) diminishes the number of symptomatic infectious individuals in human population (as shown in Fig. 9(a)). Furthermore, the use of quintuple intervention minimizes the number of infectious rodents as well as the total rodent population (see Figs. 9(b) and 9(c), respectively). To achieve this optimal solutions, combination of all controls $u_1(t)$, $u_2(t)$, $u_3(t)$, $u_4(t)$ and $u_5(t)$ requires maximal use of controls $u_1(t)$, $u_2(t)$, $u_3(t)$ and $u_4(t)$ for 23 days, 49 days, 3 days and 20 days, respectively, while control $u_5(t)$ is held at about 0.31 (31%) for almost full implementation period (as Fig. 9(d) shows).

Furthermore, the efficiency and cost-effectiveness analyses conducted in Sect. 5 suggest that implementation of optimal use of condom averts the highest number of LF infections in the interacting human and rodent populations with the efficiency of 45.374%, and the intervention strategy is also regarded the most cost-effective strategy among the five single control interventions under consideration. The least efficient and cost-effective single intervention is the application of optimal educational campaign policy. Also, combination of optimal environmental fumigation with pesticide and optimal use of condom is the most efficient (with efficiency of 99.689%) and most cost-effective double intervention among the five different double control interventions examined in this paper. Combination of optimal environmental fumigation and rodent reduction control is the least efficient and cost-effective double intervention. For triple interventions, combination of optimal environmental fumigation, optimal condom usage and rodent reduction control is not only the most efficient triple intervention, but also the most cost-effective triple intervention among the five various triple interventions analysed. The triple intervention which combines optimal environmental fumigation, optimal rodent reduction control and optimal educational campaign does not only avert

the least number of LF infections (with efficiency of 19.162%), but also regarded the least cost-effective triple intervention. For quadruple interventions, combination of optimal environmental fumigation, optimal condom usage, optimal rodent reduction control and optimal educational campaign is the most efficient quadruple intervention, while the combination of optimal environmental fumigation, optimal use of condom, optimal use of antiviral therapy and optimal educational campaign is the most cost-effective quadruple intervention among the five quadruple interventions examined. Combination of optimal environmental fumigation, optimal use of antiviral therapy, optimal rodent reduction control and optimal educational campaign is regarded the least efficient and cost-effective quadruple intervention. Finally, determination of the overall most efficient and cost-effective strategies from the set of single, double , triple, quadruple and quintuple control interventions under consideration reveals that the quintuple control intervention (combination of optimal environmental fumigation, optimal condom usage, optimal use of antiviral therapy, optimal rodent reduction control and optimal educational campaign) is the overall most efficient control intervention with 99.813% efficient, whereas the double intervention which combines optimal environmental fumigation and optimal condom usage is the overall most cost-effective control intervention.

7. Conclusion

In this work, five time-dependent control variables, namely, environmental fumigation, condom use, use of antiviral drug therapy, rodent reduction control and educational campaign, are incorporated into an existing nonlinear mathematical LF model featuring vertical mode of transmission, nonlinear incidence functions and effect of socio-economic factors such as community hygiene to investigate the best optimal control strategy for the minimization of transmission dynamics of the disease in the population at minimal cost. Using Pontryagin's maximum principle, the new optimal control framework is analysed to show the existence and characterization of the control quintuple. The impacts of various set of single, double, triple, quadruple and quintuple interventions implementation on LF transmission and spread dynamics in the interacting human and rodent populations are evaluated through numerical simulations of the optimality system. The epidemiological insights from the results show that all the implemented interventions produce positive impact in reducing the disease burden in the population compared to when no intervention is in place. In particular, we adopt EA and CEA (ICER in particular) to identify the most efficient and most cost-effective intervention, respectively. EA suggests that the use of quintuple control (combination of all the five controls) is the most efficient intervention, while CEA shows the most cost-effective single, double, triple and quadruple interventions for controlling the community spread of LASV. More importantly, CEA reveals that double intervention combining environmental fumigation with condom use is the overall most cost-effective intervention. Therefore, the most efficient quintuple intervention is recommended when resources are available. However, adoption of the most cost-effective intervention (double intervention which combines environmental fumigation and condom use) is highly recommended when the resources are limited. Alternatively, each of the most cost-effective single, double, triple and quadruple interventions may be adopted for effective and optimal control of LF in case of limited available resources.

Acknowledgements

The authors are thankful to the handling editor and the anonymous reviewers for their constructive comments and suggestions that led to the presentation of this improved manuscript.

Author contributions

All the authors contributed equally to this work, and approved the final manuscript draft.

Competing interests

The authors have no competing interests that are relevant to the contents of this article to declare.

References

Abdulhamid, A., Hussaini, N., Musa, S. S., and He, D. (2022). Mathematical analysis of Lassa fever epidemic with effects of environmental transmission. *Results Phys*, *35*, 105335. doi:https://doi.org/10.1016/j.rinp.2022.105335.

Abdullahi, A. (2021). Modelling of transmission and control of Lassa fever via Caputo fractional-order derivative. *Chaos Solitons Fractals*, *151*, 111271. doi:https://doi.org/10.1016/j.chaos.2021.111271.

Abidemi, A., and Aziz, N. A. B. (2022). Analysis of deterministic models for dengue disease transmission dynamics with vaccination perspective in Johor, Malaysia. *Int J Appl Comput Math*, *8*, 1–51. doi:https://doi.org/10.1007/s40819-022-01250-3.

Abidemi, A., Olaniyi, S., and Adepoju, O. A. (2022a). An explicit note on the existence theorem of optimal control problem. In *Journal of Physics: Conference Series* (p. 012021). IOP Publishing volume 2199. doi:https://doi.org/10.1088/1742-6596/2199/1/012021.

Abidemi, A., Owolabi, K. M., and Pindza, E. (2022b). Modelling the transmission dynamics of Lassa fever with nonlinear incidence rate and vertical transmission. *Physica A*, *597*, 127259. doi:https://doi.org/10.1016/j.physa.2022.127259.

Alade, T. O. (2021). On the generalized Chikungunya virus dynamics model with distributed time delays. *Int J Dyn Control*, *9*, 1250–1260.

Alkahtani, B. S. T., and Alzaid, S. S. (2020). Mathematical model of Lassa fever spread: Model with new trends of differential operators. *Results Phys*, *19*, 103523. doi:https://doi.org/10.1016/j.rinp.2020.103523.

Anggriani, N., and Beay, L. K. (2022). Modeling of COVID-19 spread with self-isolation at home and hospitalized classes. *Results Phys*, *36*, 105378.

Asamoah, J. K. K., Okyere, E., Abidemi, A., Moore, S. E., Sun, G.-Q., Jin, Z., Acheampong, E., and Gordon, J. F. (2022). Optimal control and comprehensive cost-effectiveness analysis for COVID-19. *Results Phys*, (p. 105177). doi:https://doi.org/10.1016/j.rinp.2022.105177.

Asamoah, J. K. K., Owusu, M. A., Jin, Z., Oduro, F. T., Abidemi, A., and Gyasi, E. O. (2020). Global stability and cost-effectiveness analysis of COVID-19 considering the impact of the environment: using data from Ghana. *Chaos Solitons Fractals*, *140*, 110103.

Asma, A., Khan, M. A., Iskakova, K., Al-Duais, F. S., and Ahmad, I. (2022). Mathematical modeling and analysis of the SARS-Cov-2 disease with reinfection. *Comput Biol Chem*, *98*, 107678.

Asogun, D. A., Günther, S., Akpede, G. O., Ihekweazu, C., and Zumla, A. (2019). Lassa fever: epidemiology, clinical features, diagnosis, management and prevention. *Infect Dis Clin*, *33*, 933–951.

Atangana, A. (2015). A novel model for the Lassa hemorrhagic fever: deathly disease for pregnant women. *Neural Comput Appl*, *26*, 1895–1903. doi:https://doi.org/10.1007/s00521-015-1860-9.

Barua, S., Dénes, A., and Ibrahim, M. A. (2021). A seasonal model to assess intervention strategies for preventing periodic recurrence of Lassa fever. *Heliyon*, *7*, e07760.

Bell-Kareem, A. R., and Smither, A. R. (2021). Epidemiology of Lassa fever. In R. Ahmed, S. Akira, A. Casadevall, J. E. Galan, A. Garcia-Sastre, B. Malissen, and R. Rappuoli (Eds.), *Current Topics in Microbiology and Immunology* (pp. 1–23). Berlin, Heidelberg: Springer. doi:https://doi.org/10.1007/82_2021_234.

Cantor, S. B., and Ganiats, T. G. (1999). Incremental cost-effectiveness analysis: the optimal strategy depends on the strategy set. *J Clin Epidemiol*, *52*, 517–522.

Eberhardt, K. A., Mischlinger, J., Jordan, S., Groger, M., Günther, S., and Ramharter, M. (2019). Ribavirin for the treatment of Lassa fever: A systematic review and meta-analysis. *Int J Infect Dis*, *87*, 15–20.

Falowo, O. D., Olaniyi, S., and Oladipo, A. T. (2022). Optimal control assessment of rift valley fever model with vaccination and environmental sanitation in the presence of treatment delay. *Model Earth Syst Environ*, (pp. 1–15). doi:https://doi.org/10.1007/s40808-022-01508-1.

Faniran, T. S., and Ayoola, E. O. (2022). Investigating essential factors in the spread of Lassa fever dynamics through sensitivity analysis. *Int J Nonlinear Anal Appl*, *13*, 485–497.

Fleming, W. H., and Rishel, R. W. (1975). *Deterministic and stochastic optimal control*. New York, Springer.

Ghosh, J. K., Ghosh, U., Biswas, M., and Sarkar, S. (2019). Qualitative analysis and optimal control strategy of an SIR model with saturated incidence and treatment. *Differ Equ Dyn Syst*, (pp. 1–15).

Gibb, R., Moses, L. M., Redding, D. W., and Jones, K. E. (2017). Understanding the cryptic nature of Lassa fever in West Africa. *Pathog Glob Health*, *111*, 276–288.

Goyal, M., Baskonus, H. M., and Prakash, A. (2019). An efficient technique for a time fractional model of Lassa hemorrhagic fever spreading in pregnant women. *Eur Phys J Plus*, *134*, 482. doi:https://doi.org/10.1140/epjp/i2019-12854-0.

Higazy, M., El-Mesady, A., Mahdy, A., Ullah, S., and Al-Ghamdi, A. (2021). Numerical, approximate solutions, and optimal control on the deathly Lassa hemorrhagic fever disease in pregnant women. *J Funct Spaces*, *2021*, 1–15.

Ibrahim, M. O., Ahiaba, A. A., and Akinyemi, S. T. (2021). Optimal control of Lassa fever quarantine model. *J Math Sci Comput Math*, *2*, 217–226. doi:https://doi.org/10.15864/jmscm.2203.

Jain, S., and Atangana, A. (2018). Analysis of Lassa hemorrhagic fever model with non-local and non-singular fractional derivatives. *Int J Biomath*, *11*, 1850100.

Lenhart, S., and Workman, J. T. (2007). *Optimal control applied to biological models*. London: CRC Press.

Lingas, G., Rosenke, K., Safronetz, D., and Guedj, J. (2021). Lassa viral dynamics in non-human primates treated with favipiravir or ribavirin. *PLoS Comput Biol*, *17*, e1008535.

Mari Saez, A., Cherif Haidara, M., Camara, A., Kourouma, F., Sage, M., Magassouba, N., and Fichet-Calvet, E. (2018). Rodent control to fight Lassa fever: Evaluation and lessons learned from a 4-year study in Upper Guinea. *PLoS Negl Trop Dis*, *12*, e0006829.

Mishra, A. M., Purohit, S. D., Owolabi, K. M., and Sharma, Y. D. (2020). A nonlinear epidemiological model considering asymptotic and quarantine classes for SARS CoV-2 virus. *Chaos Solitons Fractals*, *138*, 109953.

Musa, S. S., Yusuf, A., Bakare, E. A., Abdullahi, Z. U., Adamu, L., Mustapha, U. T., and He, D. (2022). Unravelling the dynamics of Lassa fever transmission with differential infectivity: Modeling analysis and control strategies. *Math Biosci Eng*, *19*, 13114–13136. doi:https://doi.org/10.3934/mbe.2022613.

Naik, P. A., Zu, J., and Owolabi, K. M. (2020). Global dynamics of a fractional order model for the transmission of HIV epidemic with optimal control. *Chaos Solitons Fractals*, *138*, 109826.

Ogunmiloro, O. M. (2022). Modeling the dynamics of the consequences of demographic disparities in the transmission of Lassa fever disease in Nigeria. *Model Earth Syst Environ*, (pp. 1–16). doi:https://doi.org/10.1007/s40808-022-01522-3.

Ojo, M. M., Benson, T. O., Shittu, A. R., and Doungmo Goufo, E. F. (2022). Optimal control and cost-effectiveness analysis for the dynamic modeling of Lassa fever. *J Math Comput Sci*, *12*, 136.

Omame, A., Rwezaura, H., Diagne, M., Inyama, S., and Tchuenche, J. (2021). COVID-19 and dengue co-infection in Brazil: optimal control and cost-effectiveness analysis. *Eur Phys J Plus*, *136*, 1–33.

Onah, I. S., Collins, O. C., Madueme, P.-G. U., and Mbah, G. C. E. (2020). Dynamical system analysis and optimal control measures of Lassa fever disease model. *Int J Math Math Sci*, *2020*.

Paul, A. K., and Kuddus, M. A. (2022). Mathematical analysis of a COVID-19 model with double dose vaccination in Bangladesh. *Results Phys*, *35*, 105392.

Peter, O. J., Abioye, A. I., Oguntolu, F. A., Owolabi, T. A., Ajisope, M. O., Zakari, A. G., and Shaba, T. G. (2020). Modelling and optimal control analysis of Lassa fever disease. *Inform Med Unlocked*, *20*, 100419.

Pontryagin, L. S., Boltyanskii, V. G., Gamkrelidze, R. V., and Mishchenko, E. F. (1962). *The Mathematical Theory of Optimal Processes*. Interscience, New York.

Purushotham, J., Lambe, T., and Gilbert, S. C. (2019). Vaccine platforms for the prevention of Lassa fever. *Immunol Lett*, *215*, 1–11.

Rector, C. R., S, C., and J, D. (2005). *Principles of Optimization Theory*. New Delhi: Narosa Publishing House.

Smither, A. R., and Bell-Kareem, A. R. (2021). Ecology of Lassa virus. In R. Ahmed, S. Akira, A. Casadevall, J. E. Galan, A. Garcia-Sastre, B. Malissen, and R. Rappuoli (Eds.), *Current Topics in Microbiology and Immunology* (pp. 1–20). Berlin, Heidelberg: Springer. doi:`https://doi.org/10.1007/82_2020_231`.

Tuite, A. R., Watts, A. G., Kraemer, M. U., Khan, K., and Bogoch, I. I. (2019). Potential for seasonal Lassa fever case exportation from Nigeria. *Am J Trop Med Hyg*, *100*, 647.

Wiley, M. R., Fakoli, L., Letizia, A. G., Welch, S. R., Ladner, J. T., Prieto, K., Reyes, D., Espy, N., Chitty, J. A., Pratt, C. B. et al. (2019). Lassa virus circulating in liberia: a retrospective genomic characterisation. *Lancet Infect Dis*, *19*, 1371–1378.

Yaro, C. A., Kogi, E., Opara, K. N., Batiha, G. E.-S., Baty, R. S., Albrakati, A., Altalbawy, F., Etuh, I. U., and Oni, J. P. (2021). Infection pattern, case fatality rate and spread of Lassa virus in Nigeria. *BMC Infect Dis*, *21*, 1–9.

Zhao, S., Musa, S. S., Fu, H., He, D., and Qin, J. (2020). Large-scale Lassa fever outbreaks in Nigeria: quantifying the association between disease reproduction number and local rainfall. *Epidemiol Infect*, *148*, 1–12.